AFRL-OSR-VA-TR-2014-0150

(YIP) Information Collection and Fusion for Space Situational Awareness

Puneet Singla
The Research Foundation of SUNY on behalf of Univ at BuffaloSponsored Projects Services
402 Crofts Hall
Buffalo, NY-14260-7016

06-30-2014
Final Report

Air Force Research Laboratory
AF Office Of Scientific Research (AFOSR)/RTB1

REPORT DOCUMENTATION PAGE

Form Approved
OMB No. 0704-0188

PLEASE DO NOT RETURN YOUR FORM TO THE ABOVE ORGANIZATION.

1. REPORT DATE *(DD-MM-YYYY)*	2. REPORT TYPE	3. DATES COVERED *(From - To)*
06-30-2014	Final Report	04/01/2011-03/31/2014

4. TITLE AND SUBTITLE
(YIP) Information Collection and Fusion for Space Situational Awareness

5a. CONTRACT NUMBER

5b. GRANT NUMBER
FA9550-11-1-0012

5c. PROGRAM ELEMENT NUMBER

6. AUTHOR(S)
Puneet Singla

5d. PROJECT NUMBER

5e. TASK NUMBER

5f. WORK UNIT NUMBER

7. PERFORMING ORGANIZATION NAME(S) AND ADDRESS(ES)
The Research Foundation of SUNY on behalf of Univ at Buffalo

8. PERFORMING ORGANIZATION REPORT NUMBER

9. SPONSORING/MONITORING AGENCY NAME(S) AND ADDRESS(ES)
Sponsored Projects Services
402 Crofts Hall
Buffalo, NY-14260-7016

10. SPONSOR/MONITOR'S ACRONYM(S)

11. SPONSOR/MONITOR'S REPORT NUMBER(S)

12. DISTRIBUTION/AVAILABILITY STATEMENT

13. SUPPLEMENTARY NOTES

14. ABSTRACT

A significant progress has been made towards characterizing non-Gaussian state density function. Two new methods adaptive Gaussian mixture model (AGMM) and conjugate unscented transformation (CUT) have been developed for this purpose. AGMM method solves the Fokker-Planck-Kolmogorov equation associated with orbital dynamics model. Furthermore, sparse approximation tools have been used to identify the Gaussian kernels which best approximate the state pdf. The CUT methodology provides efficient means to compute higher order moments of state density functions. The primary objective of CUT methodology is to find a fully symmetric sigma/cubature point set with reduced number of points that is equivalent to the set of cubature points of Gaussian quadrature product rule of same order. Equivalent to same order implies that for a polynomial of order 2m-1 in generic N-dimensions, both the new reduced sigma point set from the proposed method known as Conjugate Unscented Transform method (CUT) and the m^N quadrature points from the Gaussian quadrature product rule result in same order of relative percentage error. In this work, a closed form expression for these new sets of point is provided to satisfy up to 8 central moments. It is shown that th

15. SUBJECT TERMS

16. SECURITY CLASSIFICATION OF:			17. LIMITATION OF ABSTRACT	18. NUMBER OF PAGES	19a. NAME OF RESPONSIBLE PERSON
a. REPORT	b. ABSTRACT	c. THIS PAGE			19b. TELEPHONE NUMBER *(Include area code)*

Reset

1 Final Report

This report documents the major project findings during the duration of the AFOSR Young Investigator Program titled *Information Collection and Fusion for Space Situation Awareness.* The principal goals of this on-going research work are threefold:

1. To understand how uncertain input variables such as geometric properties of RSO and atmospheric drag or solar radiation pressure (SRP) coefficient and random stochastic forcing affect the output of a dynamical model for orbit propagation.

2. To estimate orbit states together with quantitative measures of confidence associated with those estimates by combining system prediction with observations from various resources.

3. To design robust methodology for optimal sensor management while taking into account the uncertainties in the system dynamics.

The highlights of the achievements of this research work are described as follows:

2 Adaptive Gaussian Mixture Model:

A major part of this research work focused on developing an approach to improve the statistical validity of Resident Space Objects (RSO) orbit estimates and uncertainties as well as a method of associating observations with the correct RSO and classifying events in near real time. Our approach involved studying an adaptive Gaussian mixture model (AGMM) solution to the Fokker-Planck-Kolmogorov Equation (FPKE) for its applicability to the RSO tracking problem. The FPKE describes the time-evolution of stochastic systems and the Adaptive Gaussian Sum Filter (AGSF) is a solution to the equation that allows for non-Gaussian pdfs. The AGSF algorithm is designed to be scalable, relatively efficient for solutions of this type, and able to handle the nonlinear effects which are common in the estimation of RSO orbit states. In addition, techniques for data association that are compatible with the AGSF based on entropy theory were examined. The AGSF and corresponding observation association methods were evaluated using simulated data to determine their performance and feasibility. The key idea of the AGSF is to approximate the state pdf by a finite sum of Gaussian density functions whose mean and covariance are propagated from one time-step to the next using linear theory. The weights of the Gaussian kernels are updated at every time-step by requiring the sum to satisfy the FPKE. When properly formulated, the mixture problem in the AGSF can be solved efficiently and accurately using convex optimization solvers, even if the mixture model includes many terms. This methodology effectively decouples a large uncertainty propagation problem into many small problems. As a consequence, the solution algorithm can be parallelized on most High Performance Computing (HPC) systems. Finally, a Bayesian framework can be used on the AGSF structure to assimilate (noisy) observational data with model forecasts.

There is no doubt that number of Gaussian kernels in the mixture model approximation plays an important role in its accuracy and computational complexity. Adaptive Gaussian Sum Mixture (AGMM) method to solve the Fokker-Planck-Kolmogorov Equation (FPKE) has been modified to automatically select number of Gaussian kernels based upon FPKE error feedback. Critical Gaussian kernels are identified which needs to be split and merged for better mixture approximation. Furthermore, sparse approximation tools ($\mathcal{L}_1$ norm minimization) have been used to obtain a compact representation of the mixture model.

Figure 1 shows the contours of the RSO orbital state pdf at different time. The RSO orbit corresponds to low Earth orbit at an altitude of 700km. Atmospheric drag and first harmonic of non-sphercal gravity Initial pdf was approximated using one Gaussian component having mean $\boldsymbol{\mu}_0$ and covariance $\boldsymbol{\Sigma}_0$.

$$\boldsymbol{\mu}_0 = [7000\ 0\ 0\ 0\ -1.0374\ 7.4771] \quad (1)$$

$$\boldsymbol{\Sigma}_0 = \text{diag}\left(0.01, 0.01, 0.01, 0.000001, 0.000001, 0.000001\right) \quad (2)$$

The initial mean and covariance were propagated for 6 hours using the equations of unscented Kalman filter. Number of Gaussian kernels in mixture approximation were automatically selected by making use of adaptive split and merge strategy in conjunction with Kullbeck-Leibler measure. 125000 monte carlo runs were used as truth to verify the developed approach. Figure 1 shows the contours of the pdf at different time. One can see that the initial Gaussian pdf characterised by circular contour evolves into non-Gaussian pdf over time. The contours of the pdf match with the contours of the monte carlo run. One can also see the change in the number of components at different time as a result of split and merge technique.

The findings of this work are disseminated through following publications:

- K. Vishwajeet, P. Singla and M. Jah, "Nonlinear Uncertainty Propagation for Perturbed Two-Body Orbits," *AIAA Journal of Guidance, Control and Dynamics*, Accepted, January 2014, DOI: 10.2514/1.G000472.
- K. Vishwajeet and P. Singla, "Adaptive Split and Merge Technique for Gaussian Mixture Models to Solve Kolmogorov Equation," *2014 American Control Conference, Portland, OR, June 4–6, 2014.*
- K. Vishwajeet and P. Singla, "Adaptive Split and Merge Algorithm for Gaussian Mixture Models," *2013 Astrodynamics Specialist Conference, Hilton Head, North Carolina*.
- K. Vishwajeet and P. Singla, "Sparse Approximation Based Gaussian Mixture Model Approach for Uncertainty Propagation for Nonlinear Systems," *2013 American Control Conference, Washington D.C.*
- K. Vishwajeet "Adaptive Gaussian Mixture Model for Uncertainty Propagation Through Perturbed Two-Body Model," *M.S. thesis, Department of Mechanical & Aerospace Engineering, University at Buffalo, Buffalo, NY, August 2013.* (**Best M.S. Thesis Award from NAGS**).
- G. Terejanu, P. Singla, T. Singh and P. Scott, "Adaptive Gaussian Sum Filter for Nonlinear Bayesian Estimation," *IEEE Transactions on Automatic Control,* Vol. 56, Issue 9, pp. 2151–2156, Sep. 2011, DOI: 10.1109/TAC.2011.2141550.

3 Conjugate Unscented Transform:

The problem of uncertainty characterization in nonlinear systems subject to stochastic excitation and uncertain initial conditions is of central interest to various domains of science and engineering. One may be interested in predicting the probability of collision of an asteroid with Earth, control of movement and planning of actions of autonomous systems, diffusion of toxic materials through atmosphere, the optimization of financial investment policies, or simply the computation of the prediction step in the implementation of a Bayes' filter. All these applications require the study of the relevant stochastic system and involve computing multi-dimensional expected value integrals with respect to an appropriate probability density function (pdf). Analytical expressions for these multi-dimension integrals in general exist for linear systems. For

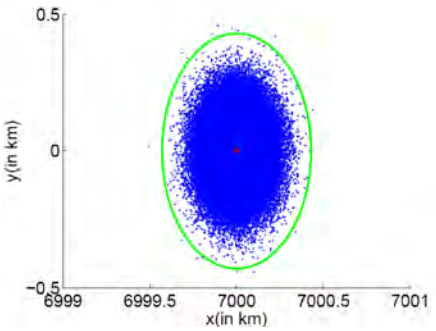

(a) pdf contours in XY plane at t = 0

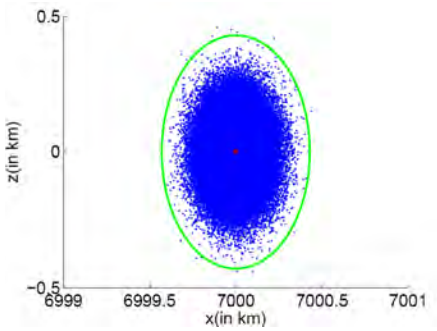

(b) pdf contours in XZ plane at t = 0

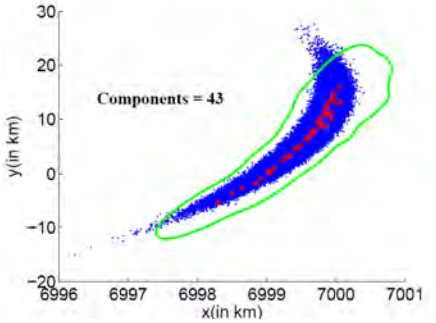

(c) pdf contours in XY plane at 3.2 hr

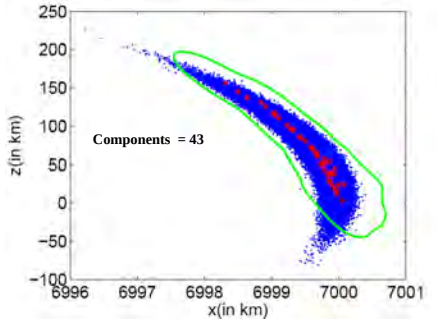

(d) pdf contours in XZ plane at 3.2 hr

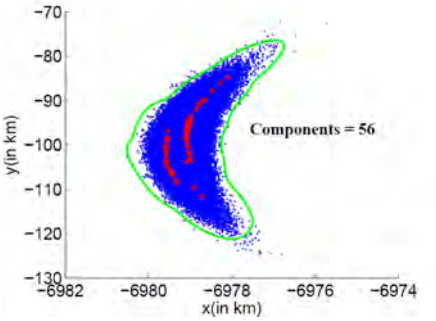

(e) pdf contours in XY plane at 4 hr

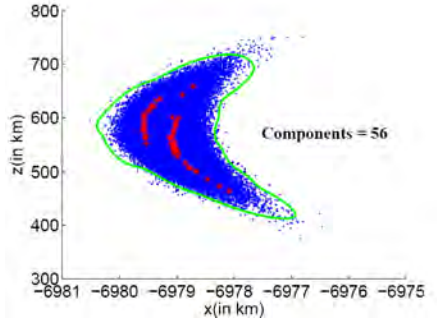

(f) pdf contours in XZ plane at 4 hr

Figure 1: Contours corresponding to prior pdf in cartesian coordinates with drag using MC(cots) & AGSF(thick line) at different time('*' indicates the centres of components)

example, the well celebrated Kalman filter provides the analytical expressions for the mean and covariance of the states of the linear system subject to Gaussian white noise and Gaussian initial condition errors. However in most other cases one often does not have direct analytical solution for these integrals and has to approximate integral values by making use of computational methods.

Several computation techniques exist in the literature to approximate the expectation integral with respect to a Gaussian pdf, the most popular being Monte Carlo (MC) methods, Gauss-Hermite (GH) Quadrature Rules, Sparse Grid quadratures such as Gauss-Hermite Smolyak (GHS) quadratures, Unscented Transformation (UT) and Cubature methods. All these methods involve an approximation of the expectation integral as a weighted sum of integrand values at specified points within the domain of integration. These methods basically differ from each other in the generation of these specific points. For example, MC methods involve random samples from the specified pdf while the Gaussian quadrature scheme involves deterministic points carefully chosen to reproduce exactly the integrals for polynomials. Quadrature rules in higher dimensions are usually referred to as cubature rules. A cubature rule is said to be *exact to degree* d, if it can only integrate all polynomials with degree $\leq d$. For $1\mathbb{D}$ (1-Dimensional) integrals, one needs n quadrature points according to the Gaussian quadrature scheme to exactly reproduce the expectation integrals of polynomials with degree $2n-1$ or less. However, in generic N$\mathbb{D}$, one needs to take the tensor product of n-$1\mathbb{D}$ quadrature points and hence would yield a total of n^N quadrature points. This cubature rule is referred to as Gaussian Quadrature Product rule. Even for a moderate-dimension system involving 6 random variables, the number of points required to evaluate the expectation integral with only 5 points along each direction is $5^6 = 15,625$. This is a non-trivial number of points that might make the calculation of the integral computationally expensive, especially when the evaluation of function at each cubature point itself can be an expensive procedure, e.g., one may need to solve a system of partial differential equations to compute the function of interest. The sparse grid quadratures or Smolyak quadrature schemes in particular take the sparse product of $1\mathbb{D}$ quadrature rules and thus have fewer points than the equivalent Gaussian quadrature rules at the cost of introducing negative weights. But fortunately the Gaussian quadrature rule is *not minimal* for $N \geq 2$ and there exists cubature rules with reduced number of points. This forms the motivation for the work presented in this paper.

In the perspective of nonlinear filtering where the integrals with Gaussian probability density functions frequently arise, cubature methods such as the UKF with reduced number of points have tremendous potential especially in an online scenario. The highly acclaimed Unscented Transform (UT) with only $2N+1$ points is a degree 3 cubature method, where these cubature points were called *sigma points*. Similar to the UT method, a more recent development is the Cubature Kalman filter (CKF) which is again exact to degree 3 but uses only $2N$ points. It can be noticed that the sigma/cubature points of $2N+1$ UT and $2N$ CKF can be observed as special cases of a more general structure of cubature points previously presented in for symmetrical probability density functions.

In this research work, a new methodology is developed to efficiently evaluate expectation integrals in general N-dimensional space by satisfying higher order moment constraint equations. New sets of cubature/quadrature points are defined to satisfy moment equations up to the tenth order. The developed methodology can be used as an efficient alternative to Gaussian quadrature rule with significantly reduced number of function evaluations while maintaining accuracy. The proposed methodology extends the main idea of the conventional unscented transformation method to construct a fully symmetric reduced sigma/cubature point set with all positive weights that sum up to one and are equivalent to the Gaussian quadrature product rule of same order. In a numerical context, equivalent to same order implies that for a polynomial of order $2m-1$ in N-dimensions, both the new reduced sigma points from the proposed method known as Conjugate Unscented Transform method (CUT) and the m^N quadrature points from the Gaussian quadrature product

rule result in same order of relative percentage error. The main idea of the CUT approach is to judiciously select specific structures for sigma points rather than taking tensor product of 1-D points like in the Gauss quadrature scheme. This allows us to compute multi-dimension expectation integrals with the same orders of magnitude in terms of error but achieves this with a far less number of points.

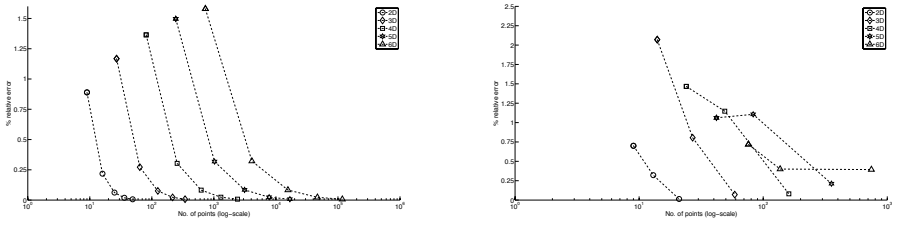

(a) Gauss-Hermite Convergence

(b) CUT Convergence

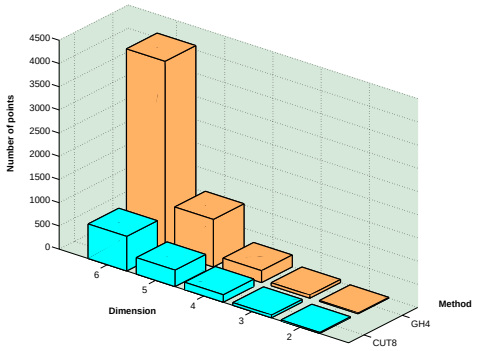

(c) Number of points required to achieve 0.5% Rel. error

Figure 2: GH vs. CUT: Simulation Results corresponding to $f(\mathbf{X}) = (\sqrt{1 + \mathbf{X}^T\mathbf{X}})^{-3}$

Fig. 2(a) shows the relative error with respect to the true value of the following expectation integral as a function of GH quadrature points along each dimension while varying the dimension of input space from 2 to 6.

$$E[f(\mathbf{X})] = \int (\sqrt{1 + \mathbf{X}^T\mathbf{X}})^{\alpha}, \mathbf{X} \in \mathbb{R}^N \, \mathbf{x0}_{N\times 1} 0.1 I_{N\times N} d\mathbf{x} \tag{3}$$

This is a benchmark problem and it had been discussed that computing the expectation of $f(\mathbf{X})$ for negative values for α is a challenging task since $\alpha < 0$ leads to a delta-sequence functions. Taking, $\alpha = -3$ and the identity covariance of the zero mean Gaussian pdf is scaled down by 0.1 to make the integral value converge with reasonable number of points. Similarly, Fig. 2(b) shows the relative error for dimensions 2 to 6 using the CUT methods. Furthermore, Fig. 2(c) shows the minimal number of points required for each method to achieve at least 0.5% relative error. It is clear that the proposed CUT8 method yields the accuracy of 0.5% as the GH4 quadrature rule but with much smaller fraction of the number of points.

One could take advantage of these cubature rules in the evaluation of the integrals while maintaining higher accuracy and thus feasible on-line execution of a filter. To illustrate the effectiveness of the proposed approach, let us consider a typical air traffic control scenario as shown in Figure 3(a). The kinematics of the turning motion is modeled by the set of nonlinear equations called 'CT'- Coordinated Turn. The CT model is characterized by constant speed and constant turn rate. The turn rate Ω is usually unknown and

is hence appended to the state vector making the model nonlinear. The system dynamic equations for CT-model, where the state vector $x = [\xi \quad \dot{\xi} \quad \eta \quad \dot{\eta} \quad \Omega]^T$ and sensor model that consists of a radar located at the origin and measures the range and bearing are:

$$x_k = \begin{bmatrix} 1 & \frac{sin(\Omega T)}{\Omega} & 0 & -\frac{1-cos(\Omega T)}{\Omega} & 0 \\ 0 & cos(\Omega T) & 0 & -sin(\Omega T) & 0 \\ 0 & \frac{1-cos(\Omega T)}{\Omega} & 1 & \frac{sin(\Omega T)}{\Omega} & 0 \\ 0 & sin(\Omega T) & 0 & cos(\Omega T) & 0 \\ 0 & 0 & 0 & 0 & 1 \end{bmatrix} x_{k-1} + \nu_{k-1}, \qquad \begin{bmatrix} r_k \\ \theta_k \end{bmatrix} = \begin{bmatrix} \sqrt{(\xi_k)^2 + (\eta_k)^2} \\ tan^{-1}(\frac{\eta_k}{\xi_k}) \end{bmatrix} + \omega_k \tag{4}$$

The process noise ν_k and measurement noise ω_k are independent zero mean gaussian noise processes with following covariance matrices:

$$Q_{k-1} = L_1 \begin{bmatrix} \frac{T^3}{3} & \frac{T^2}{2} & 0 & 0 & 0 \\ \frac{T^2}{2} & T & 0 & 0 & 0 \\ 0 & 0 & \frac{T^3}{3} & \frac{T^2}{2} & 0 \\ 0 & 0 & \frac{T^2}{2} & T & 0 \\ 0 & 0 & 0 & 0 & \frac{L_2}{L_1} T \end{bmatrix}, \quad R_k = \begin{bmatrix} \sigma_r^2 & 0 \\ 0 & \sigma_\theta^2 \end{bmatrix} \tag{5}$$

The parameters used in the simulation are given as: $\begin{matrix} T = 5s & L_1 = 0.16 & \sigma_r = 100\,m \\ T_f = 495s & L_2 = 0.01 & \sigma_\theta = 1degree \end{matrix}$ The initial condition uncertainty is:

$$x_0 = [25000\,m, \ -120\,m/s, \ 10000\,m, \ 0\,m/s, \ 0.000001\,rad/s]^T \tag{6}$$

$$P_{0/0} = diag([1000^2\,m^2, \ 100\,m^2/s^2, \ 1000^2\,m^2, \ 100\,m^2/s^2, \ (1\pi/180)^2\,rad^2/s^2]) \tag{7}$$

The filters used in the simulations are listed below:

Cubature Kalman Filter (CKF)- with 10 points	Unscented Kalman Filter (UKF) - with 11 points
CUT4- with 42 points	CUT6- with 83 points
CUT8- with 355 points	GH6 - with 7776 points
Particle Filter (PF)- with 5000 sample points	

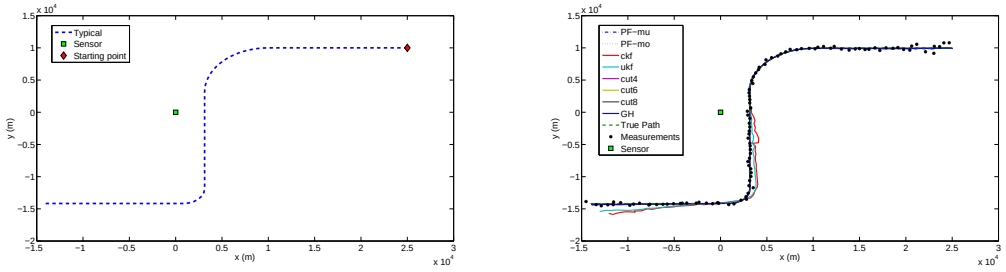

(a) Airplane Trajectory (b) Filter Estimates

Figure 3: Simulation Results for Air-Traffic Scenario

A simulation of all these filters are shown in Figure 3(b). The trajectories of each filter shown in the Figure 3(b) is the average over 200 runs.

As the dimension of the process model is 5, to avoid a negative weight in the UT a kappa value of $\kappa = 1$ is considered. Each run consists of randomly selecting a point from initial distribution as the initial condition for the filters, generating the measurements from the true trajectory by the sensor model (4) and random noise with covariance R. All the filters are initiated with the same initial point and use the same set of measurements for a particular run. A batch of 200 runs are performed for each filter considered. The root mean square error RMSE in position,velocity and turn rate for the batch of runs is calculated for each filters as follows

$$RMSE_{pos}(k) = \sqrt{\frac{1}{200}\sum_{i=1}^{200}((\xi_i(k) - \hat{\xi}_i(k))^2 + (\eta_i(k) - \hat{\eta}_i(k))^2)} \tag{8}$$

$$RMSE_{vel}(k) = \sqrt{\frac{1}{200}\sum_{i=1}^{200}((\dot{\xi}_i(k) - \dot{\hat{\xi}}_i(k))^2 + (\dot{\eta}_i(k) - \dot{\hat{\eta}}_i(k))^2)} \tag{9}$$

$$RMSE_{\Omega}(k) = \sqrt{\frac{1}{200}\sum_{i=1}^{200}((\Omega_i(k) - \hat{\Omega}_i(k))^2} \tag{10}$$

The RMSE in position and velocity is calculated individually for each filter estimate with respect to the true trajectory. The 2-norm in the RMSE is calculated as:

$$\|RMSE_{pos}\|_2 = \sqrt{\sum_{k=1}^{n_{T_f}} RMSE_{pos}(k)^2}, \qquad \|RMSE_{vel}\|_2 = \sqrt{\sum_{k=1}^{n_{T_f}} RMSE_{vel}(k)^2} \tag{11}$$

where n_{T_f} is the number time steps in the simulation. Table 1 gives a quick summary of the 2-norms in the RMSE errors. Illustrative figures are also shown to compare the various filters. The $RMSE_{pos}$ is shown in Figures 4(a)- 4(d). For the sake of readability, Figure 4(a) shows the performance of all the filters while the rest of the Figures 4(b)-4(d) show the same results but with different combinations of filters to avoid the overlap of the results of different filters. In the figures 'PF-mu' denotes the mean estimate of the particle filter while 'PF-mo' represents the mode estimate of the particle filter. One can see that the estimates of the Particle filter mean and mode are very close. One can see the gradual improvement as the order of the filters are increased. CKF and UKF being 3rd order rules have the maximum error. While the results of CUT8 and GH6 are very much comparable to the particle filter.

Table 1: Comparison of 2-norms of RMSE in position, velocity and turn rate

$\|\|RMSE\|\|_2$ *in*	$PF-mean$	$PF-mode$	CKF	UKF	$CUT4$	$CUT6$	$CUT8$	$GH6$
$Position$	2655.80	2843.22	23028.35	16414.90	4251.00	3151.78	3044.16	2982.91
$Velocity$	544.38	810.77	374946.32	317452.34	119231.01	58900.37	776.35	895.45
Ω	0.8842	1.6476	63.4233	53.7346	26.4342	19.2502	2.0175	2.2820

Finally, this newly developed method is tested for the orbit uncertainty characterization for low Earth object. For simulation purposes, we consider a satellite in Low Earth Orbit (LEO) at an altitude of $622\,km$. The initial state probability density function (pdf) of the system is assumed to be Gaussian with the following

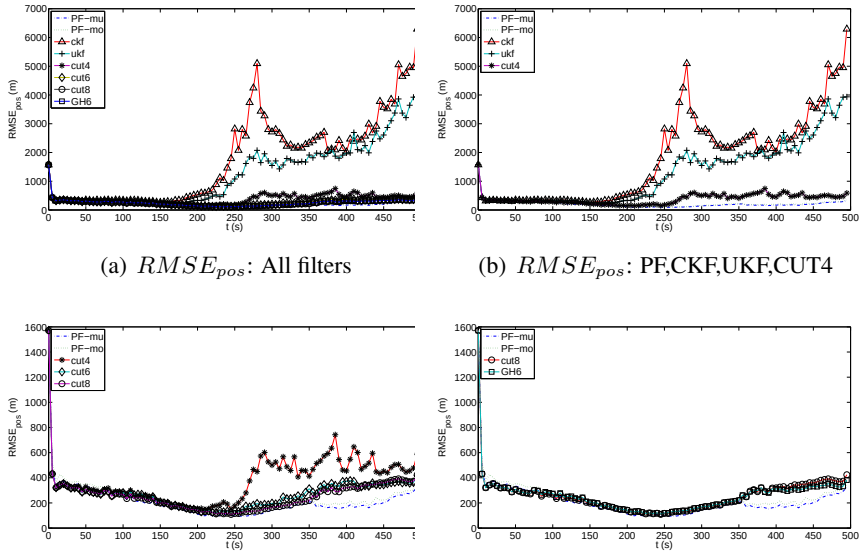

(a) $RMSE_{pos}$: All filters

(b) $RMSE_{pos}$: PF,CKF,UKF,CUT4

(c) $RMSE_{pos}$: PF,CUT4,CUT6,CUT8

(d) $RMSE_{pos}$: PF,CUT8,GH6

Figure 4: Comparison of $RMSE_{pos}$ with Particle Filter Results

mean (in km) and covariance (in km^2):

$$\boldsymbol{\mu}_0 = \begin{bmatrix} 7 \times 10^3 \\ 0 \\ 0 \\ 0 \\ -1.0374 \\ 7.4771 \end{bmatrix} \qquad \mathbf{P}_0 = \begin{bmatrix} 0.01 & 0 & 0 & 0 & 0 & 0 \\ 0 & 0.01 & 0 & 0 & 0 & 0 \\ 0 & 0 & 0.01 & 0 & 0 & 0 \\ 0 & 0 & 0 & 0.000001 & 0 & 0 \\ 0 & 0 & 0 & 0 & 0.000001 & 0 \\ 0 & 0 & 0 & 0 & 0 & 0.000001 \end{bmatrix}$$

The covariance matrix reflects a standard deviation of $100m$ in the initial estimate of the three position coordinates and a standard deviation of $1m/s$ in the estimate of velocity. The time period of the satellite is 0.8104 hours. Exponential atmospheric density model was considered to evaluate atmospheric drag term. Furthermore, first harmonic of non-spheric gravity field, J_2 was also considered. To assess the accuracy of CUT, we consider 100,000 Monte Carlo (MC) runs to be ground truth and compare first four moments computed through CUT to with those computed through MC runs. There are 3, 6, 10 and 15 distinct first order, second order, third order and fourth order moments. At each time time t, the 2-norm in the error of each moment is taken with respect to the corresponding moment calculated by 100,000 MC runs. These are then denoted as $M_1(t)$, $M_2(t)$, $M_3(t)$ and $M_4(t)$. The values are further scaled by the radius of the Earth and the 2-norm over time is taken. The results are shown in Table 2. From these results, it is clear that CUT methodology capture the moments of non-Gaussian pdf with a order of magnitude less points. *This really demonstrate the efficacy of the newly developed CUT approach in capturing non-Gaussian behavior with very few model runs.*

Furthermore, the principle of maximum entropy is used to approximate orbit state pdf from moments computed through CUT points. Figure 5 shows the marginalized pdfs in (x, y) and (x, z) respectively using the MC sample points in 3D. It can be seen that by using only moments upto order 2, the resultant pdf is Gaussian that tends to neglect the tail region of the pdf. As higher order moments are considered, the tail

Table 2: Error in moments (x,y,z) with respect to 100,000 MC runs

Moment	MC	UT	CUT4	CUT6	CUT8
$\|\|M_1(t)/Re\|\|_2$	0.0015	0.0003	0.0003	0.0003	0.0003
$(\|\|M_2(t)/Re\|\|_2)^{1/2}$	0.4802	0.1635	0.1650	0.1650	0.1650
$(\|\|M_3(t)/Re\|\|_2)^{1/2}$	0.7034	2.0967	1.3654	1.3654	1.3654
$(\|\|M_4(t)/Re\|\|_2)^{1/2}$	7.7290	16.4402	3.8991	3.8833	3.8833
No. of Points	10000	13	76	137	745

region is better captured. The marginalized pdfs using CUT4 points are shown in Figure 6. The marginalized pdfs using CUT6 points are shown in Figure 7. The CUT6 points show improvement compared to the CUT4 points and very much the same as the one obtained by MC runs. This once again reiterate the significance of newly developed CUT approach in capturing non-Gaussian behavior.

Furthermore, a test case is considered to show the efficacy of the proposed approach in approximating the probability of collision between two satellites. The initial conditions are chosen such that at the point of closest approach, the pdf of one satellite is significantly non Gaussian. The satellite initial condition state vectors of the form $[x\ km, y\ km, z\ km, \dot{x}\ km/s, \dot{y}\ km/s, \dot{z}\ km/s]$ are taken as

$$\mu_1 = [7000, 0, 0, 1.0374, -1.0374, 7.4771] \tag{12}$$

$$\mu_2 = [6729.4309, -318.1595, -1381.8922, 2.2649, -1.1893, 7.1694] \tag{13}$$

$$P_1 = [0.01, 0.01, 0.01, 1e^{(-9)}, 1e^{(-9)}, 1e^{(-9)}] \tag{14}$$

$$P_2 = [0.01, 0.01, 0.01, 1e^{(-8)}, 1e^{(-8)}, 1e^{(-8)}] \tag{15}$$

The first satellite is propagated for $1, 72, 860$ seconds while the second satellite is propagated for $21, 600$ seconds. The satellite that is propagated for over two days has significant non-gaussian nature. For example, Figure 8 shows a snapshot of 100,000 Monte Carlo runs when the random point clouds of both satellites intersect. As the time of closest approach is itself a random variable, one does not know the exact time of maximum probability of conjunction. Hence, the conjunction probability is evaluated for ± 20 second time interval from the time of closest approach calculated from the nominal (mean) trajectories of the two satellites.

Figure 9 shows the probability of collision computed through various methods. 2.3 million Monte Carlo (MC) samples are considered to provide ground truth. The full non Gaussian conjunction probability computed via the principle of maximum entropy closely agrees with the MC probability. Further, the Gaussian approximation significantly underestimates the probability by an order of magnitude. These preliminary results provides the basis for optimism for the proposed idea.

The findings corresponding to this work are disseminated through following publications:

- N. Adurthi, and P. Singla, "A Conjugate Unscented Transformation Based Approach for Accurate Conjunction Analysis," *Richard Battin Special Issue of the AIAA Journal of Guidance, Control, and Dynamics, In Preparation*.

- N. Adurthi and P. Singla, "Principle of Maximum Entropy for Probability Density Reconstruction: An Application to the Two Body Problem," *2013 Astrodynamics Specialist Conference, Hilton Head, SC, August 2013.*

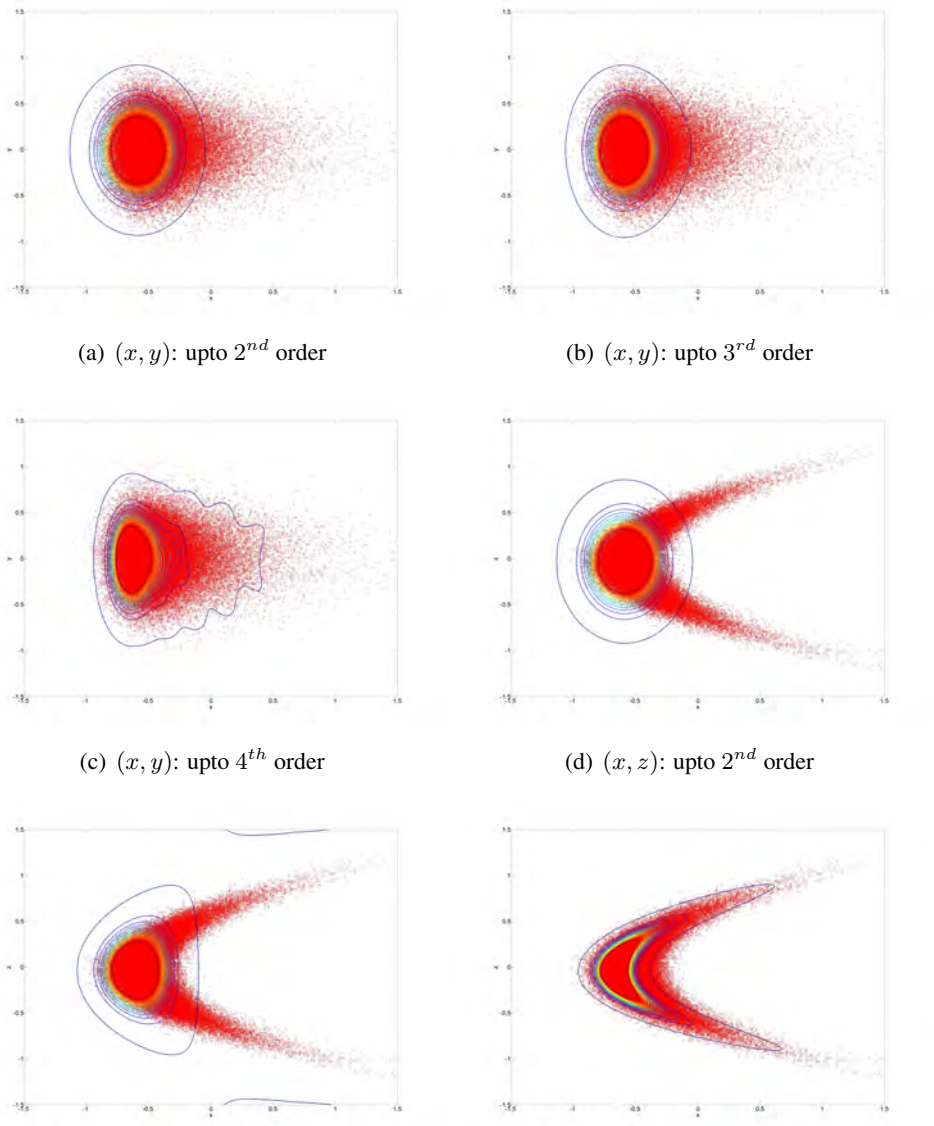

(a) (x, y): upto 2^{nd} order

(b) (x, y): upto 3^{rd} order

(c) (x, y): upto 4^{th} order

(d) (x, z): upto 2^{nd} order

(e) (x, z): upto 3^{rd} order

(f) (x, z): upto 4^{th} order

Figure 5: MC: Marginalized pdf reconstruction using all 3D moments

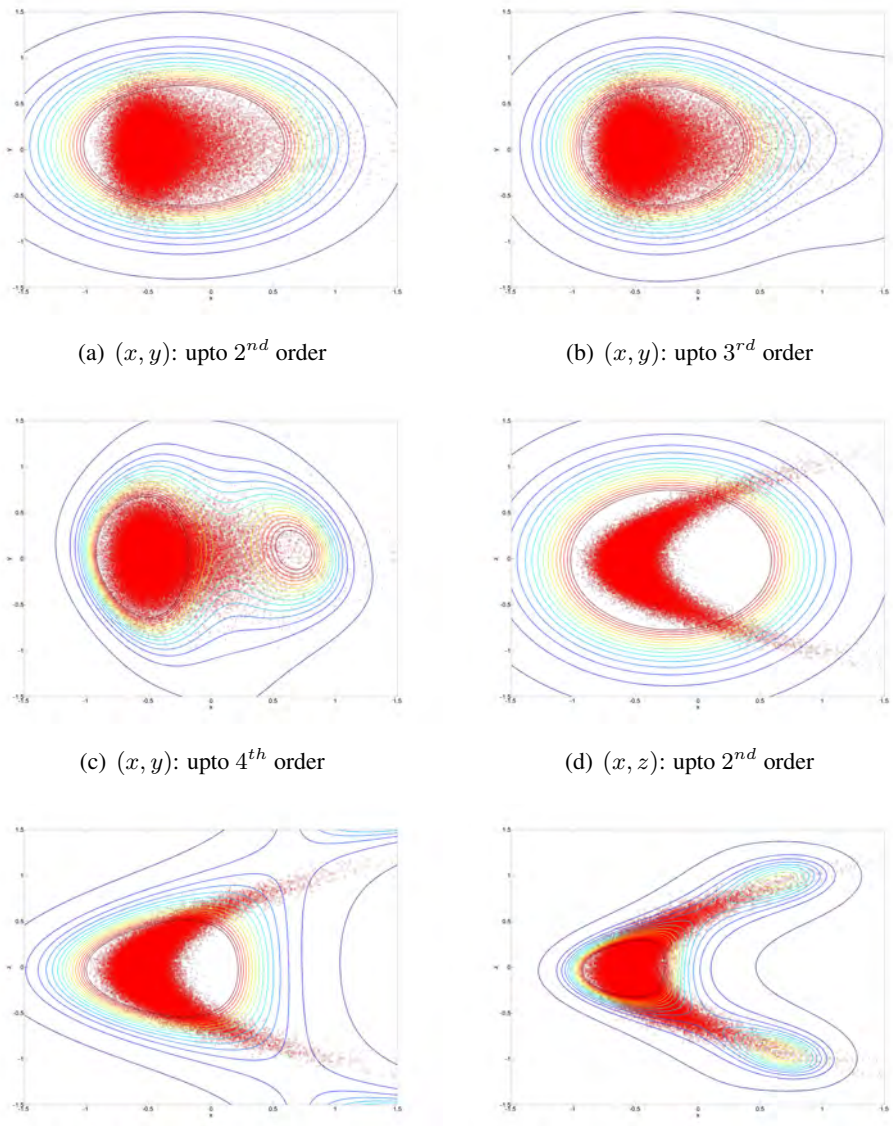

(a) (x, y): upto 2^{nd} order

(b) (x, y): upto 3^{rd} order

(c) (x, y): upto 4^{th} order

(d) (x, z): upto 2^{nd} order

(e) (x, z): upto 3^{rd} order

(f) (x, z): upto 4^{th} order

Figure 6: CUT4: Marginalized pdf reconstruction using all 3D moments

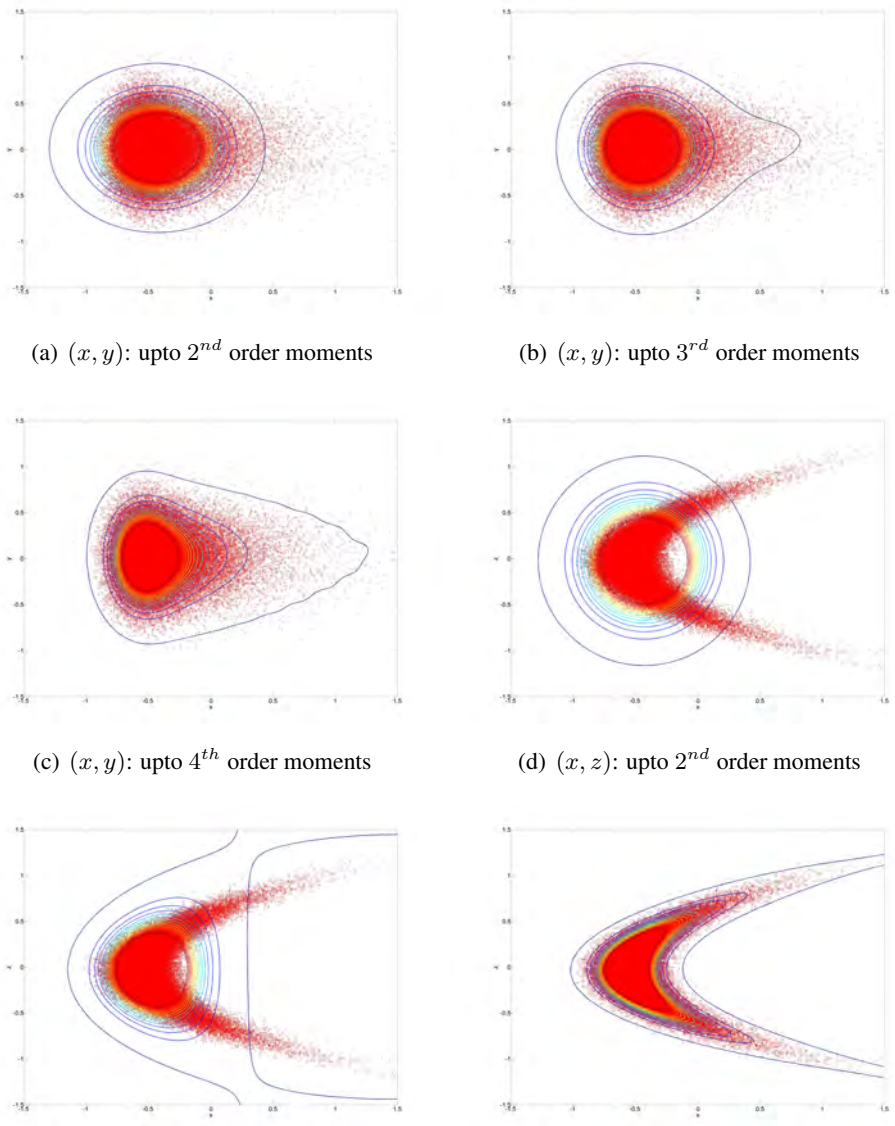

(a) (x, y): upto 2^{nd} order moments

(b) (x, y): upto 3^{rd} order moments

(c) (x, y): upto 4^{th} order moments

(d) (x, z): upto 2^{nd} order moments

(e) (x, z): upto 3^{rd} order moments

(f) (x, z): upto 4^{th} order moments

Figure 7: CUT6: Marginalized pdf reconstruction using all 3D moments

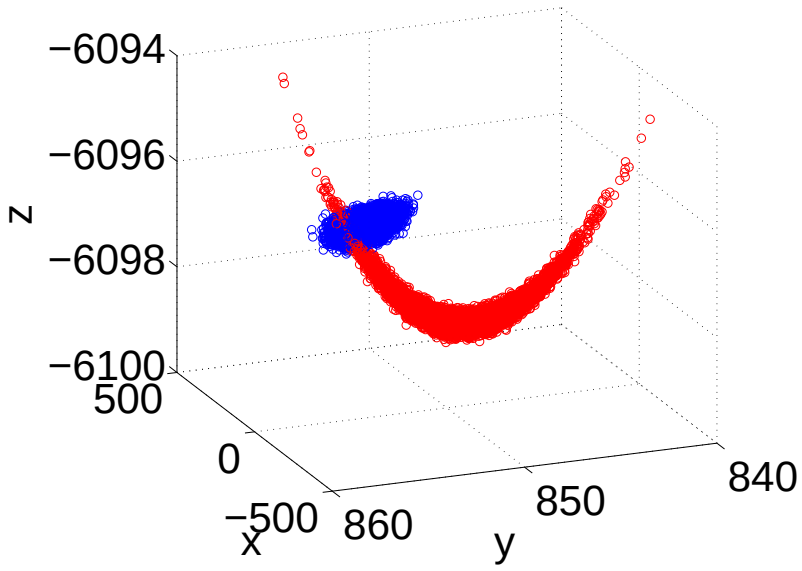

Figure 8: Snapshots: Probable collision in the tail of the density function.

- N. Adhurthi, P. Singla and T. Singh, "Conjugate Unscented Transform: a novel cubature approach for nonlinear transformation of moments in forecasting and estimation," *IEEE Transactions on Automatic Control, In Review*.
- N. Adurthi and P. Singla, "Principle Of Maximum Entropy For Probability Density Reconstruction: An Application To The Two Body Problem," *2013 AAS/AIAA Astrodynamics Specialist Conference*.
- N. Adurthi, "Conjugate Unscented Transformation Approach for Filtering and Bayesian Inference," *M.S. thesis, Department of Mechanical & Aerospace Engineering, University at Buffalo, Buffalo, NY, August 2013.* (**Best M.S. Thesis Award from NAGS**).
- N. Adurthi, P. Singla and T. Singh, "Conjugate Unscented Transform Rules for Uniform Probability Density Functions," *2013 American Control Conference, Washington D.C.*
- N. Adurthi, P. Singla and T. Singh, "Conjugate Unscented Transform and its Application to Filtering and Stochastic Integral Calculation," *2012 AIAA Guidance, Navigation & Control Conference, Minneapolis, MN.*
- N. Adurthi, P. Singla and T. Singh, "The Conjugate Unscented Transform - An Approach to Evaluate Multi-Dimensional Expectation Integrals," *2012 American Control Conference, Montréal, Canada, June 27-June 29, 2012.*
- N. Adurthi, P. Singla and T. Singh, "Conjugate Unscented Transformation "Optimal Quadrature"," *2012 SIAM Conference on Uncertainty Quantification, Raleigh, NC, April 2–April 5, 2012.*

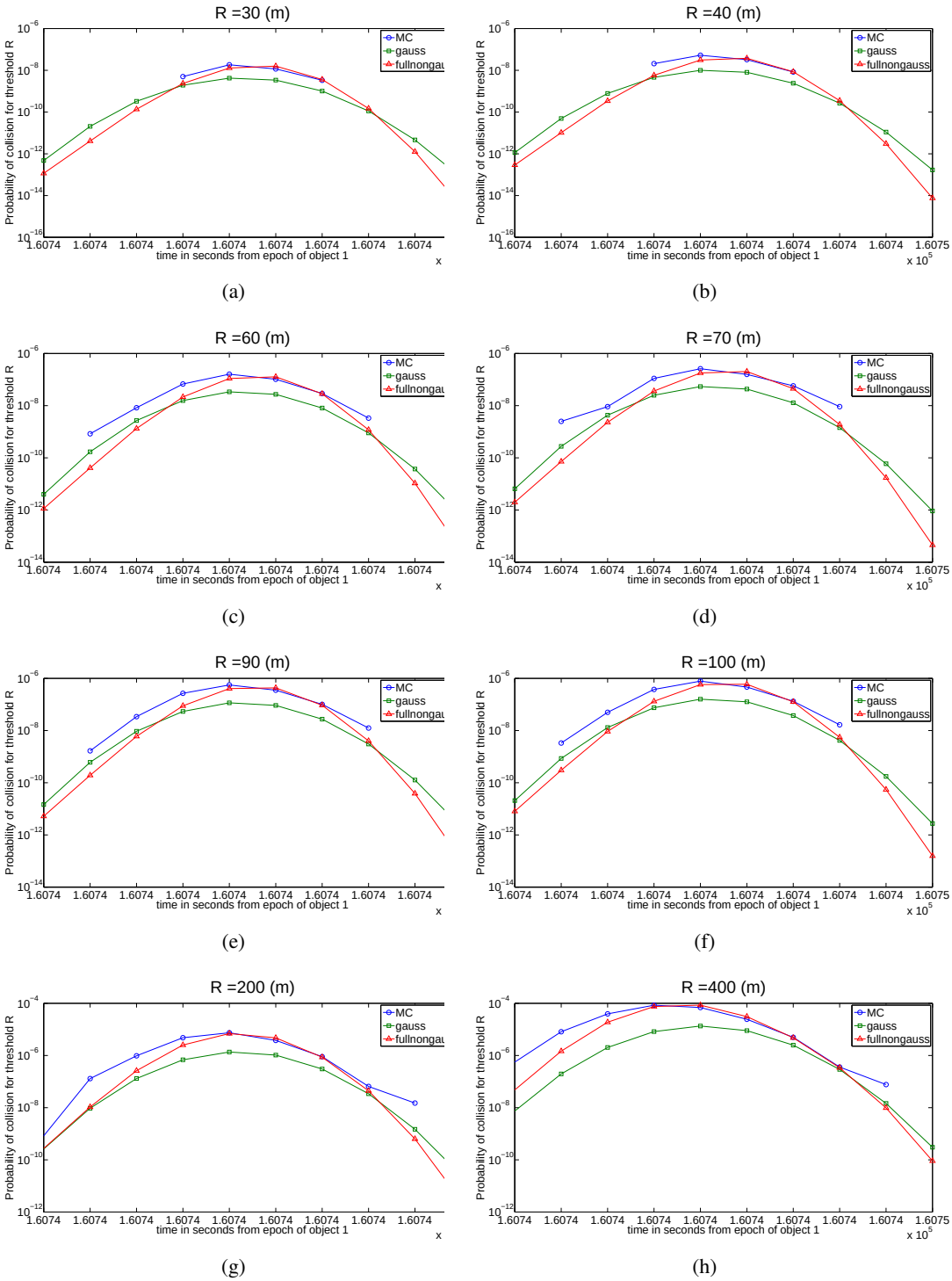

Figure 9: Probability of Collision Computed Through Various Methods

4 Efficient Conjunction Analysis:

Interactions of and with space debris and Resident Space Objects (RSOs) has emerged as a significant danger to most space operations. Current technology allows for the tracking of debris down to approximately five centimeters and from this, a catalog of over 21,000 objects currently in orbit has been generated. Because of the large number of RSOs and the limited number of sensors available to track these objects, it is impossible to maintain persistent surveillance on all objects, and, therefore there is inherent uncertainty and latency in the catalog. Although small, the high velocities obtained by the debris in low-earth orbit (LEO) and geosynchronous orbit (GEO) warrants a risk of high damage to satellites and other man-made objects. The examination of this risk, typically referred to as conjunction analysis, is a computationally-intensive process due to the amount of RSOs considered. A recent incident in February 2009 involving an unintentional collision between Russia's Cosmos 2251 satellite and a US Iridium satellite clearly illustrate the need for effective conjunction analysis. This collision resulted in over 500 pieces of debris which pose an additional risk to other space assets. Brute force conjunction analysis algorithms has combinatorial computational complexity and hence require $O(N^2)$ computations, where N is the number of RSOs considered, and typically rely on numerical simulations of a mathematical model of the underlying physics of the orbital debris. These simplified methods, however, do not account for uncertainty in the location of the debris.

Standard conjunction analysis involves the acquisition of several quantities including the time of closest approach, the relative distance between the objects in question, and the probability of collision. A preliminary step is often taken to rule out any conjunctions. In this case, the geometric location of two objects is used to show that the objects will never cross paths. Once certain collisions are ruled out, the remaining possibilities can be investigated. The objects in question are propagated through a dynamical model, and their relative distance computed. An important step in determining potential collisions is to delineate between the orbit of each RSOs. Objects are separated by their orbital height from the surface of the Earth. In this sense, it is assumed that objects in low-Earth orbit (LEO) will not collide with objects in a geosynchronous orbit (GEO). The first step is compute the distance between the largest perigee value and the smallest apogee value from the two orbits. If this distance is less than some specified distance tolerance, then the collision of two satellites will be examined. The next step is to determine whether or not a close approach between the two satellites occurs. If a close approach has been determined, an error ellipsoid must be constructed to further assess the risk of collision. The error ellipsoid is created about the first satellite of interest using the uncertainty in the satellites location. This results in creating the ellipsoid based on the covariance matrix designated for the aforementioned satellite, and ensuring the major axis is aligned with the satellite's velocity vector. The next step in analyzing a possible collision involves determining the probability of collision of two objects.

Prior to computing the probability of collision, a close approach between two objects must be determined. From this, the next step is to compute the relative velocity vector between the two objects of interest. It is assumed that all covariance data is accurate and available at each time step. For simplicity, it is also assumed that the two objects in question are spherical to remove any attitude dependencies. Associated with each object is a covariance matrix, which is used to specify an error ellipsoid about that object. Each error ellipsoid provides n standard deviations from the mean location of the object, where the value for n is to be specified by the user depending on the desired accuracy. As it is assumed that the objects are independent and identically distributed (i.i.d), the two covariance matrices are summed to create a large $n - \sigma$ error ellipsoid, where n is the same for both objects. This error ellipsoid is centered about the first object of interest. A virtual plane termed "the encounter plane" is then formed perpendicular to the relative velocity vector, and the error ellipsoid is projected onto this plane, creating an ellipse. To represent all possible

conjunctions, the first and second objects are merged to form one spherical object, whose radius is equal to the sum of the two radii in question. This combined object is placed such that it follows the relative velocity vector. From there, the new object is projected onto the encounter plane. The probability of collision is now effectively reduced to a two-dimensional computation.

This outline provides a complete brute-force method for determining conjunctions. While complete, certain faults prevent this method from its application to all scenarios. For correct application, this method requires that the size of all objects be known. Also required is the condition that the miss distance be greater than or equal to the combined object radius. The most notable downside to this approach, however, is the computational load required to compute these conjunctions. For N objects, N^2 interactions must be considered. While this computational burden is the main motivation behind the proposed method, previous attempts have been made towards reducing the computational load of conjunction analysis.

Simple attempts such as considering only objects that fall within a specified orbit, and thus a certain distance from of one another have been made in an effort to reduce the computational load required for conjunction analysis algorithms. These efforts, however, do not take into consideration the possibility that although two objects may seem very distant from one another, the uncertainty in their locations could prove to be high, warranting a possible collision. In this research work, we introduce a hierarchical approach using a kd-tree with the aid of a probability-based distance metric known as the Hellinger distance. Such approaches have been extensively studied in the gravitational N-body problem literature. Our approach is inspired by the great efficiencies obtained by the use of hierarchical approaches and in particular kd-tree based approaches.

The nodes of a kd-tree are not physically created; they are used simply to index data points. The standard kd-tree implementation is described as "top-down" as this is the direction of construction of the tree. The root box, which can be described as the space surrounding the entire data set, is first initialized. The root box is then divided along a specified dimension, typically the longest available, creating two nodes. Once divided, the location of each data point is examined to determine their respective placement in the kd-tree - if the particle is leftward of the division, it is placed into the leftmost node, and vice versa for a rightward particle. From here, the procedure is repeated until only one particle lies in each node (box). Upon completion of the final divisions, the remaining boxes, each populated with one data point, are termed leaves. This insertion procedure is termed recursion, and it's simplicity governs the favored implementation of kd-trees. It must be noted that kd-trees do not warrant the creation of a physical mesh but rather, each division is present only to discern the location of each particle. The boxes are stored simply to index each particle. It must also be noted that while the original order of the data set is maintained, during construction of the kd-tree the data set is organized in increasing order to ensure rapid construction of the kd-tree. A simplified kd-tree algorithm is presented below:

With the kd-tree implementation discussed, the nearest-neighbor search can be examined. A standard nearest-neighbor (NN) search is conducted by computing the Euclidean distance between all possible combinations of particles. By sorting the results, the nearest neighbor to each particle can be determined. Kd-trees aid in NN searches by reducing the computational load required. The computational complexity of a standard "brute-force" NN search is $O(N^2)$ whereas a kd-tree based search reduces this load to $O(NlogN)$, where N is the number of particles considered. A kd-tree NN search algorithm is outlined below:

The standard NN search via a kd-tree implementation is clearly more efficient than a brute-force NN search algorithm, which requires the computation of the distance between all possible combinations of particles. It can immediately be seen that the kd-tree lends itself towards conjunction analysis and other particle collision applications.

Algorithm 1 Standard kd-tree Implementation

Initialize size of Root Box based on dataset.
Reorganize dataset based on median value. Note: original order is maintained elsewhere. Let p denote a single datapoint
if p$<$ $division$ **then** place p into leftmost node.
else
    place p into the rightmost node.
if node contains more than one point **then** divide node.
else
    store as leaf.
Continue until each node becomes a leaf, i.e. each node contains only one datapoint.

Algorithm 2 Kd-Tree Nearest-Neighbor Search

Determine required number of nearest neighbors.
for $p = 1$ **to** Number of points **do**
    begin
    Locate the particle of interest in the kd-tree.
    Traverse up the tree, opening boxes until the required number of nearest neighbors is met.
    Compute the distance from the particle of interest to the nearest neighbors found.
    Store the minimum distance value, d_{min}.
    Compute the distance from the particle of interest to all remaining nodes (boxes) in the kd-tree, d_{box}.
    if $d_{box} < d_{min}$ **then** open the box and compute the distance from the particle of interest to the enclosed particles. Update d_{min} and nearest neighbors.
    end

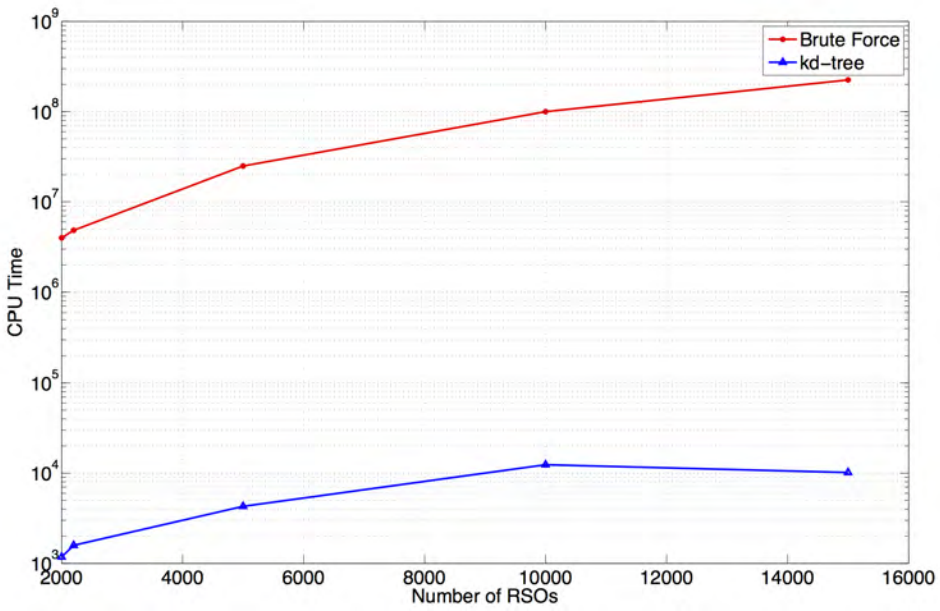

Figure 10: Comparision of Required CPU Time for Brute-Force and Kd-Tree Nearest Neighbor Searches

It must first be noted that as each particle possesses an uncertain location, the mean value of each particle is used to construct the kd-tree. The main modification appears in the NN search implementation. As opposed to using Euclidean distance, a probabilistic distance metric is to be employed to compute the distance between particles of interest. It must be noted, however, that in computing the distance between a single particle and a given node (box), the Euclidean distance metric is still employed. The interaction between two particles, however, requires a probabilistic distance metric. Here, the Kullback-Leibler divergence, the Bhattacharyya distance, and the Hellinger distance have been considered.

A preliminary result of this study is depicted in Figure 10, showing the approximate CPU time for both a brute-force and a tree-based nearest neighbor computation as a function of the number of resident space objects. It can be seen that the kd-tree based approach offers a marked improvement in the required CPU time for the modified nearest neighbor search when compared to the brute-force approach. The kd-tree method corroborated results obtained by the brute-force method, ensuring that the Hellinger distance provides a link to the actual probability of collision.

The findings corresponding to this work are disseminated through following publications:

- N. Adurthi, and P. Singla, "A Conjugate Unscented Transformation Based Approach for Accurate Conjunction Analysis," *2014 AIAA/AAS Astrodynamics Specialist Conference, San Diego, California, 4 - 7 August 2014*.
- M. Mercurio, "A Non-Combinatorial Approach for Efficient Conjunction Analysis," *M.S. Thesis, University at Buffalo, June 2014.*
- M. Mercurio and P. Singla, "A Hierarchical Tree Code Based Approach for Efficient Conjunction Analysis," *2013 Astrodynamics Specialist Conference, Hilton Head, SC, August 2013.*
- M. Mercurio, P. Singla and A. Patra, "A Hierarchical Tree Code Based Approach for Efficient Con-

junction Analysis," *2012 AIAA/AAS Astrodynamics Specialist Conference, Minneapolis, MN, Aug. 2Aug. 5, 2012.*

5 Optimal Information Collection:

Often the problem of optimally locating or configuring the sensor parameters is important as it can profoundly effect the performance of a particular sensor. For example given the uncertain nature of space debris and limited measurements or cost, one is always interested in optimally configuring/scheduling the sensors in future-time to make the 'best measurements' possible, as good measurements can lead to better decisions or improved estimates. Often in directional sensors with limited field of view (FOV) such as radar, laser, sonar or infrared ranging devices, it is important to point the sensor at the target (possibly moving). Hence, the problem of deploying and configuring such sensors with limited FOV becomes an integral part of the measurement process. The concept of sensor management is not new and is still an active field of research where many have considered various utility functions to describe sensor performance.

The problem of optimal sensor placement and motion coordination of mobile sensor networks has been addressed in target tracking literature. The objective function that measures the sensor performance is generally taken as the Fisher Information matrix (FIM). This sensor performance cost is apt as the inverse of the FIM is known as the Cramer Rao lower bound (CRLB) which is the lower bound of the covariance of the parameter estimates. As an estimate with lower covariance is always desired, minimizing this lower bound or equivalently by maximizing an appropriate norm of the FIM one can achieve desired sensor configurations. But it is emphasized that the minimization is done for a bound which intuitively implies better performance. Conventionally, following metrics for the fisher information matrix are used:

- D-optimality ($-ln\{det(FIM)\}$)
- E-optimality or maximum eigenvalue ($\lambda_{max}(FIM^{-1})$)
- A-optimality ($tr(FIM^{-1})$)
- Sensitivity criterion($-tr(FIM)$)

Recently, the principle of maximum mutual information was used for dynamic sensor selection in case of linear Gaussian models. Often information utility functions have neat analytical expressions when the underlying probability density functions(pdf) are Gaussian. For a general pdf, the problem of computing these information measures can be a challenge and hence the pdf is usually approximated by an equivalent Gaussian pdf. Gaussian approximation in some cases might not be appropriate, for example when the underlying pdf is multi-modal, a single Gaussian approximation would neglect partly or even completely the high/low probability regions.

The objective of this research work is to optimally manage various sensors configurations to tradeoff between competing indices such as energy consumption, coverage of domain and the information gathered. A suitable information reward for taking action (sensor modality and placement) can be the expected one step reduction in the total uncertainty of the system state. Due to the uncertain nature of the target with nonlinear dynamics, the evolution of cost function is essentially stochastic and hence the problem can be categorized as a stochastic optimal control problem. As the mutual information measure is generally not convex in the control variable, the problem of even solving for a numerically approximate solution is challenging and at times intractable.

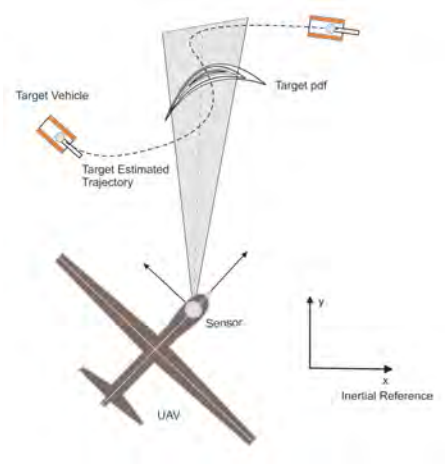

Figure 11: UAV-Sensor-Target Schematic

A generic problem scenario is depicted in Figure 11, where a controllable platform such as an Unmanned Aerial Vehicle (UAV) with a configurable sensor is to move and configure the sensor parameters such that it can make 'better' measurements of the uncertain uncooperative target. One is also interested in the cases when there are constraints on time, fuel or even the number of possible measurements. Let the dynamics of the UAV with known initial condition $\mathbf{s}_0$ be described by

$$\mathbf{s}_{k+1} = F(\mathbf{s}_k, u_k) \tag{16}$$

A reasonable assumption is made that there is no uncertainty in the UAV state dynamics. The state of the UAV typically consists of position, velocity and heading angle. The target dynamics with uncertain initial conditions $\mathbf{x}_0 \sim p(\mathbf{x}_0)$ is given by an assumed non-linear model

$$\mathbf{x}_{k+1} = f(\mathbf{x}_k) + \nu_k \tag{17}$$

where randomness in its motion is modelled by Gaussian sequence $\nu_k \sim \mathcal{N}(\nu : \mathbf{0}, \mathbf{Q}_k)$. The measurement model is a function of the states of the UAV ($\mathbf{s}$), sensor parameters (θ) and the target ($\mathbf{x}$) as the measurements are made with respect to the coordinate frame of the UAV and are then converted to the corresponding measurements in the ground reference frame.

$$\mathbf{z}_{k+1} = h(\mathbf{s}_{k+1}, \mathbf{x}_{k+1}, \theta_{k+1}) + g(\mathbf{s}_{k+1}, \mathbf{x}_{k+1}, \theta_{k+1})\omega_{k+1} \tag{18}$$

where $\omega_{k+1} \sim \mathcal{N}(\omega : \mathbf{0}, \mathbf{R}_{k+1})$.The state pdf evolves with time according to the Chapman-Kolmogorov equation (CKE). As the measurements are made at every time step the pdf of the target state is updated using Bayes' rule (BR) as

$$\begin{aligned} CKE: \quad & p(\mathbf{x}_{k+1}|\mathbf{z}_k, \mathbf{s}_k) = \int p(\mathbf{x}_{k+1}|\mathbf{x}_k) p(\mathbf{x}_k|\mathbf{z}_k, \mathbf{s}_k)\, d\mathbf{x}_k \\ BR: \quad & p(\mathbf{x}_{k+1}|\mathbf{z}_{k+1}, \mathbf{s}_k) = \frac{p(\mathbf{z}_{k+1}|\mathbf{x}_{k+1}, \mathbf{s}_k) p(\mathbf{x}_{k+1}|\mathbf{z}_k, \mathbf{s}_k)}{p(\mathbf{z}_{k+1}, \mathbf{s}_k)} \end{aligned} \tag{19}$$

The objective is to find a sequence of control inputs $[u_k, \theta_k]$ to the UAV (and mounted sensor) to minimize a particular cost function. The open loop optimal control problem can be framed as

$$Min: \ J = \psi[s_{N_T}] + \sum_{k=0}^{N_T-1} \left\{ - \underbrace{I(\mathbf{x}_k, \mathbf{z}_k|\mathbf{s}_k, \theta_k)}_{Mutual\ Information} + \underbrace{\mathbf{s}_k^T A \mathbf{s}_k + u_k^T B u_k}_{UAV\ energy} \right\} \tag{20}$$

$$\textit{constraint to}: \begin{cases} \mathbf{s}_{k+1} = F(\mathbf{s}_k, u_k) \\ p(\mathbf{x}_{k+1}) = \int p(\mathbf{x}_{k+1}|\mathbf{x}_k) p(\mathbf{x}_k)\, d\mathbf{x}_k \\ C_\theta(\theta_k) \leq 0 \quad and \quad C_u(u_k) \leq 0 \\ p(\mathbf{x}_0) \\ \mathbf{s}_0 \end{cases} \tag{21}$$

The cost function consists of two parts: Mutual Information, that is to be maximized and the energy (fuel) consumed by the UAV is to be minimized. Ideally the optimal control sequence determined at the initial time is no longer valid right after the first measurement update and a new optimal control problem needs to be solved. This might be computationally expensive to perform at every time step. Alternatively it is logical to solve a new optimal control problem only when there is significant change in the target state pdf $p(\mathbf{x}_k|\mathbf{z}_k, \mathbf{s}_k)$ at time k when compared to the predicted target pdf $p(\mathbf{x}_k)$ at time k for which the optimal control sequence was solved.

$$D_{KL}\left(p(\mathbf{x}_k|\mathbf{z}_k, \mathbf{s}_k)||p(\mathbf{x}_k)\right) \geq D_{threshold} \tag{22}$$

In this work, the principle of Dynamic Programming (DP) is adopted to solve for the optimal action/control:

$$J^*_{N_T}(\mathbf{s}_{N_T}) = \psi[s_{N_T}]$$
$$J^*_k(\mathbf{s}_k) = \min_{u_k} \left\{ -I(\mathbf{x}_k, \mathbf{z}_k|\mathbf{s}_k, \theta_k) + u_k^T B u_k + J^*_{k+1}(F_k(\mathbf{s}_k, u_k)) \right\}$$

Due to the highly nonlinear FOV constraints, information measure can change abruptly and optimization algorithms which involve gradients are usually not applicable. A discrete DP formulation is highly advantageous as the process does not involve gradients and can also be made parallel. In addition it is known that the computation time strongly depends only on the level of discretization. Thus by adding multiple targets and multiple sensors the computation time is weakly influenced. Both Adaptive Gaussian Mixture Model (AGMM) and Conjugate Unscented Transformation (CUT) are used to solve the CKE equation for the optimal control problem.

For the purpose of simulation, the sensor model equations as described in (18) is composed of the true sensor model $h(\mathbf{x}_{k+1}, \mathbf{s}_{k+1}, \theta_{k+1})$ and an assumed function $g(\mathbf{x}_{k+1}, \mathbf{s}_{k+1}, \theta_{k+1})$ that penalises the measurement made outside the FOV. Fig 12a, shows one kind of penalty $g(.)$.

In this case study, the optimal trajectory to track a moving target is sought. For this simulation the target is assumed to be an airplane with state vector $x = [\xi, \dot{\xi}, \eta, \dot{\eta}, \Omega]^T$ making a Coordinate turn (CT):

$$x_k = \begin{bmatrix} 1 & \frac{sin(\Omega T)}{\Omega} & 0 & -\frac{1-cos(\Omega T)}{\Omega} & 0 \\ 0 & cos(\Omega T) & 0 & -sin(\Omega T) & 0 \\ 0 & \frac{1-cos(\Omega T)}{\Omega} & 1 & \frac{sin(\Omega T)}{\Omega} & 0 \\ 0 & sin(\Omega T) & 0 & cos(\Omega T) & 0 \\ 0 & 0 & 0 & 0 & 1 \end{bmatrix} x_{k-1} + \nu_{k-1}, \tag{23}$$

$[\xi, \eta]$ are the position coordinates of the airplane and $[\dot{\xi}, \dot{\eta}]$ are the corresponding velocities, Ω is the turn rate. Here the $T = 1s$ is the discrete time step for the target dynamics. The assumed process noise ν_{k-1}

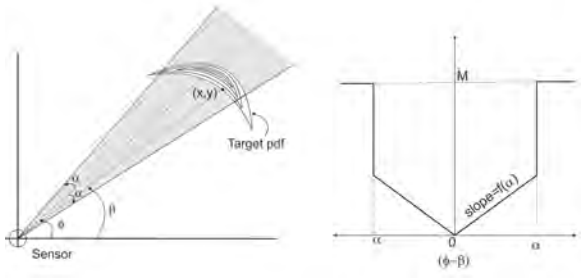

Figure 12: Sensor-Target Schematic

has covariance matrix Q_{k-1} with parameter $(L_1, L_2) = (0.02, 10^{-5})$. The measurement model consists of range and bearing angle measurements within the FOV of the sensor.

$$h(\mathbf{x}, \mathbf{s}, \theta) = \begin{bmatrix} \sqrt{(\xi - s_1)^2 + (\eta - s_2)^2} \\ tan^{-1}\left(\frac{\eta - s_2}{\xi - s_1}\right) \end{bmatrix} \tag{24}$$

The FOV consists of a circular sector with angle 60^o and radius 50m. A measurement update is performed only when the true target position falls within the FOV. The constant measurement noise covariance is $R_{k+1} = diag[0.5^2\ m^2, (1\pi/180)^2\ rad^2]$. As the measurement model is not a function of the velocity of the target, the mutual information can be computed from the marginalised pdf .The DP algorithm is initially computed for the whole simulation time i.e 25 time steps. A new optimal trajectory is computed at time step 12 when the threshold $D_{threshold}$ in eqn (22) exceeds 10 by solving the DP problem from time step $t_k = 12$ to $t_{T_f} = 25$. To calculate the information and propagate the state pdf the minimal cubature points of CUT6 are used. For this particular simulation the initial condition uncertainty is taken as $p(\mathbf{x}_0) = 0.5\mathcal{N}(\mathbf{x} : \mu_{\mathbf{1}}, P_1) + 0.5\mathcal{N}(\mathbf{x} : \mu_{\mathbf{2}}, P_2)$, where the Gaussian components represent information from two different sources. The values for the means and covariance are:

$$\begin{array}{ll} \mu_{\mathbf{1}} = [10, -1, 10, 5, -5\pi/180]^T & \mu_{\mathbf{1}} = [10, 2, 10, 3, -3\pi/180]^T \\ P_1 = diag[1, 0.5, 1, 0.5, 10^{-3}] & P2 = diag[1, 0.5, 1, 0.5, 10^{-3}] \end{array}$$

A random point from this distribution is selected as the true initial position of the target. It is emphasized that this true location along with its trajectory is unknown to the DP problem and is only used to generate random measurements when the target is in the sensor FOV, otherwise there is no measurement update of the state pdf. Fig 13(f) shows the drop in the joint entropy of the target state pdf with every measurement compared to the pure propagation of the target pdf. During the initial time steps it can be seen that there is no decrease in the uncertainty as the target pdf evolves. This is because the target is not visible to the sensor. Figs 13(a) - 13(e) show snapshots of the simultaneous motion of the sensor along the optimal trajectory and the updated state pdf of the target.

Finally, we solve an information optimization problem to manage a network of ground based sensors to maximize the mutual information on the system of space objects being observed by the network. A limited look-ahead policy is used to solve the dynamic programming problem that schedules the elements of a ground based surveillance network to maximize the mutual information. Simulation results will be used to validate the sensor management algorithms reported in the paper.

Figure 14 shows various time snapshots of the sensor management algorithm performance where 10 RSOs are tracked using 5 radar observation stations with known sensor uncertainties at various locations on the Earth. Unscented transformation is used to evaluate the FIM and computation of the mutual information performance measure for sensor management. Figure 15 shows the time history of the Frobenius norm of

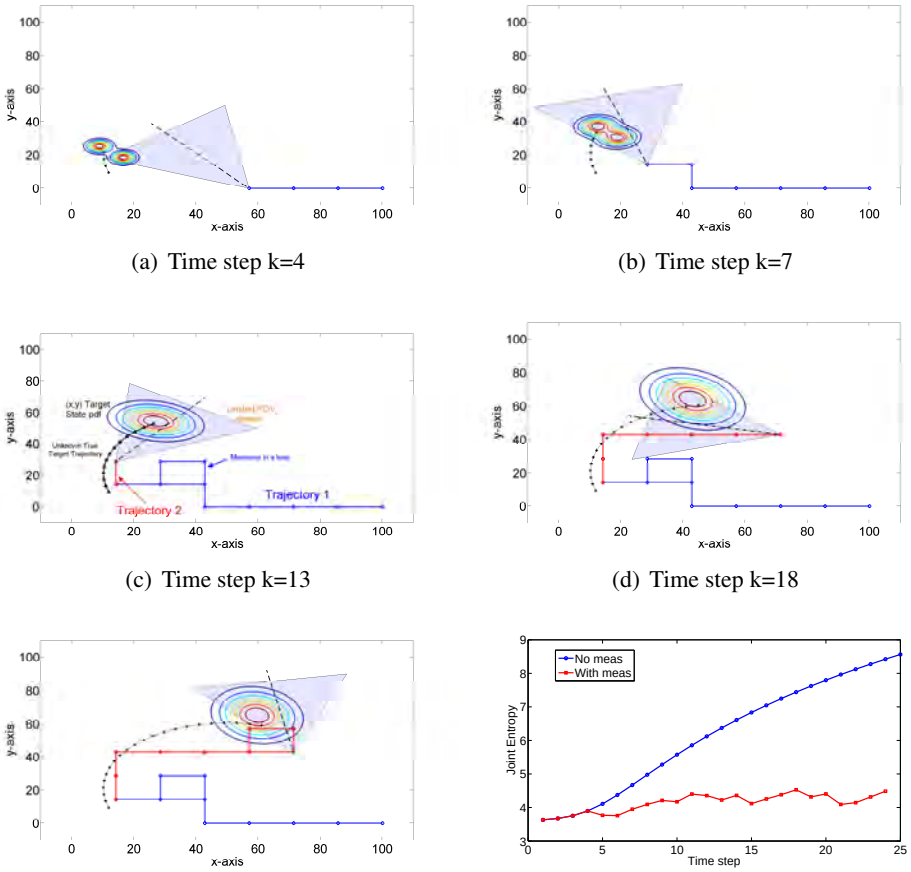

(a) Time step k=4

(b) Time step k=7

(c) Time step k=13

(d) Time step k=18

(e) Time step k=22

(f) Decrease in Joint Entropy

Figure 13: Optimal Trajectory

the covariance matrix of each object under surveillance using the optimal sensor schedule generated by our approach. The reduction of covariance of all the objects being tracked demonstrates the optimism of the technical approach discussed in the full paper. The full paper presents all the technical details of the sensor management algorithms.

The findings corresponding to this work are disseminated through following publications:

- N. Adurthi, P. Singla and M. Majji, "Optimal Sensor Tasking for Space Situational Awareness," *Richard Battin Special Issue of the AIAA Journal of Guidance, Control, and Dynamics, In Preparation.*
- N. Adurthi, P. Singla and M. Majji, "Information theoretic Optimal Sensor management for Efficient Space surveillance," *2014 AIAA/AAS Astrodynamics Specialist Conference, San Diego, California, 4 - 7 August 2014*.
- N. Adurthi and P. Singla, "Information Driven Optimal Sensor Control for Efficient Target Localization and Tracking," *2014 American Control Conference, Portland, OR, June 4–6, 2014.*
- N. Adurthi, P. Singla and T. Singh, "Optimal Information Collection for Nonlinear systems- An Appli-

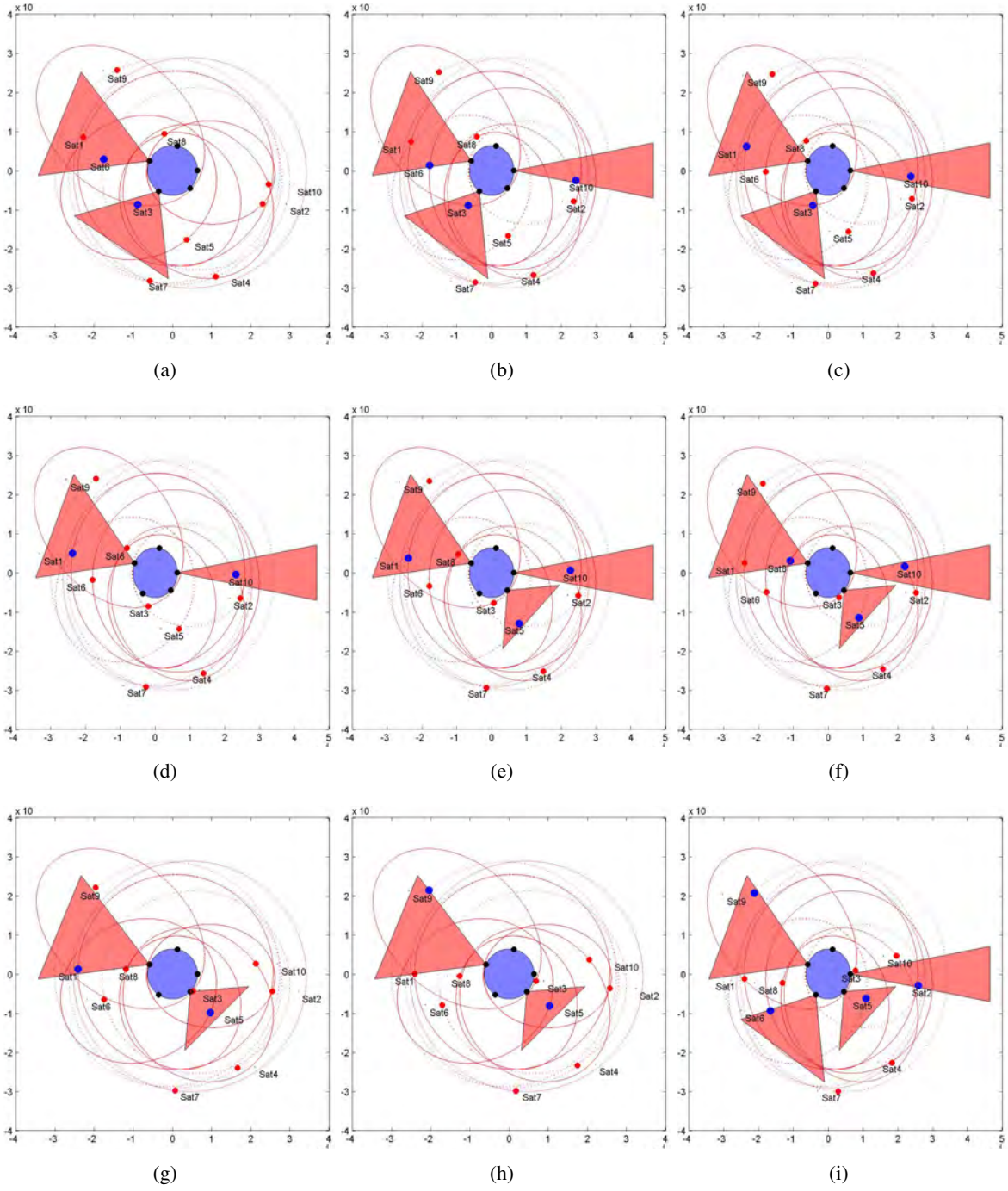

Figure 14: Snapshots of the simulation at various times

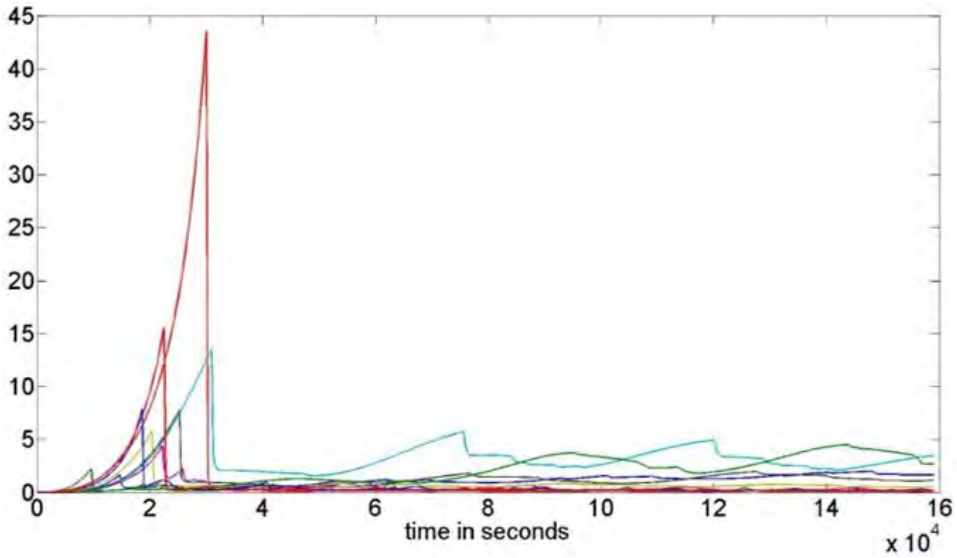

Figure 15: Reduction in Frobenius norm of covariance of each object with time

cation to Multiple Target Tracking and Localization," *2013 American Control Conference, Washington D.C.*

- R. Madankan, P. Singla and T. Singh, "Optimal Information Collection for Source Parameter Estimation of Atmospheric Release Phenomenon," *2014 American Control Conference, Portland, OR, June 4–6, 2014.*

- K. Vishwajeet, N. Adurthi and P. Singla, "Optimal Information Collection for Space Situational Awareness," *2014 SIAM Conference on Uncertainty Quantification, Savannah, GA, March 31–April 3, 2014.*

- N. Adurthi, R. Madankan and P. Singla, "Optimal Information Trajectory Design for Dynamic State Estimation," *2014 SIAM Conference on Uncertainty Quantification, Savannah, GA, March 31–April 3, 2014.*

6 Polynomial Chaos based Bayes Filter:

Two new recursive approaches have been developed to provide accurate estimates for posterior moments of both parameters and system states while making use of the generalized Polynomial Chaos (gPC) framework for uncertainty propagation. The main idea of the gPC method is to expand random state and input parameter variables involved in a stochastic differential/difference equation in a polynomial expansion. These polynomials are associated with the prior pdf for the input parameters. Later, Galerkin projection is used to obtain a deterministic system of equations for the expansion coefficients. The first proposed approach (gPC-Bayes) provides means to update prior expansion coefficients by constraining the polynomial chaos expansion to satisfy a specified number of posterior moment constraints derived from the Bayes' rule. The second proposed approach makes use of the minimum variance formulation to update gPC coefficients. The

main advantage of proposed methods is that they not only provide point estimate for the state and parameters but they also provide statistical confidence bounds associated with these estimates.

To illustrate the effectiveness of the developed ideas, let us consider the example involving the the Duffing oscillator:

$$\ddot{x} + \eta\dot{x} + \alpha x + \beta x^3 = \sin(3t) \tag{25}$$

$$\mathbf{y}(t_k) = \begin{bmatrix} x(t_k) \\ \dot{x}(t_k) \end{bmatrix} + \nu_k \tag{26}$$

For simulation purposes, nominal parameter values are assumed to be given as:

$$\eta = 1.3663,\ \alpha = -1.3761\ \beta = 2$$

The initial states are assumed to be normally distributed:

$$x(0) = \mathcal{N}(x_0| - 1, 0.25), \quad \dot{x}(0) = \mathcal{N}(\dot{x}_0| - 1, 0.25)$$

Hence, $\psi_k(\boldsymbol{\xi})'s$ are chosen to be Hermite polynomials to describe Gaussian distribution of states. As well, 4^{th} order gPC expansion is considered to analyze the effect of initial condition uncertainty.

To corroborate the efficacy of the PCQ approach to capture the evolution of the statistics of states of (25), relative error in Frobenius norm of the difference between different moments of states with respect to 10^5 Monte Carlo runs at $t = 2sec.$ is evaluated. Table 3 shows that the relative error decreases as the number of quadrature points increases. It is clear that one can obtain a better approximation for three central moments using only 16 quadrature points, relative to the 10^3 MC runs.

Table 3: Relative error in Frobenius norm of the difference between moments of states and 10^5 Monte Carlo runs at $t = 2sec.$

Number of Quadrature Points	Mean	2^{nd} Central Moment	3^{rd} Central Moment
1^2	4.5526%	100%	100%
2^2	0.3217%	20.3050%	98.3149%
3^2	0.0329%	3.9559%	28.5219%
4^2	0.0537%	0.5202%	2.5084%
10^3 MC Simulations	0.1199%	6.0715%	99.2219%

To verify the efficiency of our method, we compared the performance of the proposed methods with the extended Kalman Filter (EKF) and Particle Filter (PF) results. The measurement data is assumed to be available at a sampling frequency of 1Hz. A random sample of initial conditions is taken from initial condition distribution to generate the noise-free measurement data. The noise-free measurement data is then corrupted with a Gaussian white noise of zero mean and variance being:

$$R = \begin{pmatrix} \sigma^2 & 0 \\ 0 & \sigma^2 \end{pmatrix}$$

σ is assumed to be 0.05 in our simulations.

Fig. 16(a) and Fig. 16(b) illustrate the state estimation error for x and $\dot{x}$ by using EKF method, respectively. The solid blue line represents the difference between the true value and its mean estimate. Dashed

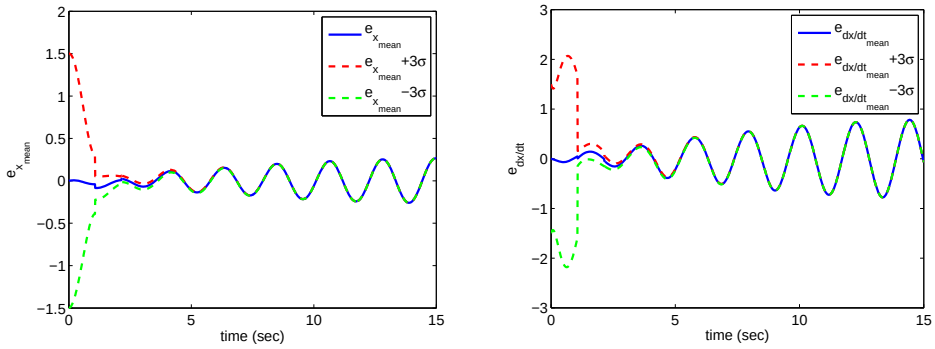

(a) $x(t)$ (b) $\dot{x}(t)$

Figure 16: Error and 3σ Bounds for the EKF Approximated Posterior Mean for Duffing oscillator

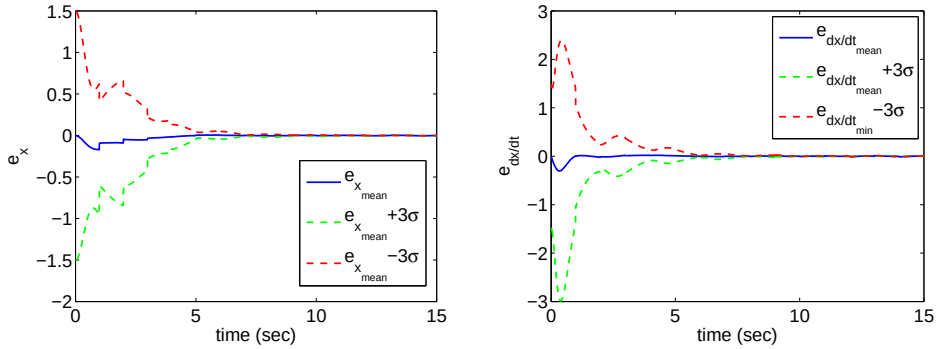

(a) $x(t)$ (b) $\dot{x}(t)$

Figure 17: Error and 3σ Bounds for PF Approximated Posterior Mean for for Duffing oscillator

green line shows -3σ bound while the dashed red line represents the 3σ bound. From these plots, it is clear that the state estimation error increases significantly with time although it is always bounded by 3σ bounds. The poor performance the EKF can be attributed to strong nonlinearities and sparse data resulting from sampling at 1 Hz.

The state estimation error for x and $\dot{x}$ by using Particle Filter have been shown Fig. 17(a) and Fig. 17(b), respectively. The solid blue line represents the difference between the true value and its mean estimate. Dashed green line shows minimum bound while the dashed red line represents the maximum bound. These plots show that the state estimation error decreases during the time, while using PF.

Furthermore, Fig. 18 shows the error in state estimates along with its 3σ bounds using the gPC based minimum variance estimator. Once again, the estimation error along with 3σ bounds converge to zero over the time which can be again attributed to the posterior density function being a delta function as number of measurements increases.

Fig. 19 shows the error in state estimates using the gPC-Bayes method for various values of N_m. The solid blue line represents the difference between the true value and its mean estimate. Dashed green line

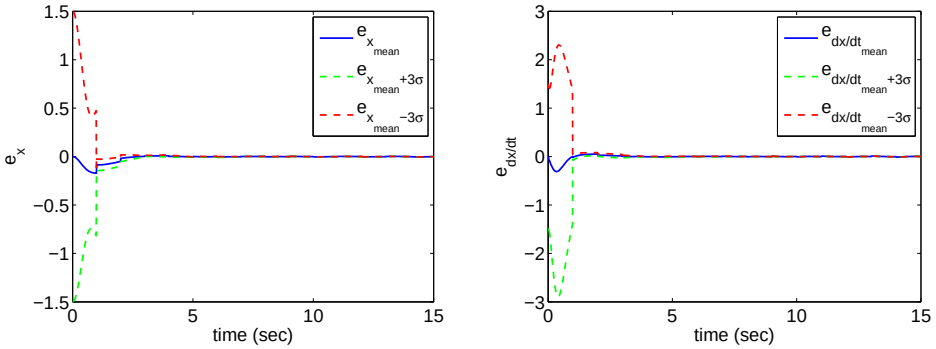

(a) $x(t)$ (b) $\dot{x}(t)$

Figure 18: Error and 3σ Bounds for the Minimum Variance Approximated Posterior Mean for Duffing oscillator

Table 4: RMSE error in mean estimate of states x and $\dot{x}$ while using different estimation methods

Method		e_x	$e_{\dot{x}}$
EKF		0.1307	0.3858
PF		0.0408	0.0508
minimum variance		0.0359	0.0527
gPC-Bayes	$N_m = 1$	0.1173	0.0695
	$N_m = 2$	0.0347	0.0531
	$N_m = 3$	0.0336	0.0528

and dashed red line represent the min and max bounds on estimation errors, respectively. It is clear that estimation error and corresponding 3σ bounds for estimation error converge to zero over the time. This is due to the fact that posterior density function finally converges to a dirac-delta function around the truth which is expected as number of measurements increases over the time. Also, it should be noticed that 3σ bounds becomes more and more tighter as one increases the number of matching moment constraints, i.e., N_m. From these results, it is clear that the proposed methods perform very well in not only estimating the posterior mean but posterior density function also.

To summarize, the root mean square error over time between the mean estimate of states and their true value has been shown in Table 4. As this table represents, gPC-Bayes and PF method perform very well in estimation of both states x and $\dot{x}$, while EKF results in high error between the mean estimate and actual value of the states. It is clear from Table 4 that by increasing the number of matching moment constraints (N_m) in gPC-Bayes method, the error in estimation of states decreases.

The findings corresponding to this work are disseminated through following publications:

- R. Madankan, P. Singla, T. Singh and P. Scott, "Polynomial Chaos Based Method for State and Parameter Estimation," *AIAA Journal of Guidance, Control and Dynamics,* Vol. 36, No. 4 (2013), pp. 1058-1074, July 2013, DOI: 10.2514/1.58377.

- R. Madankan, P. Singla, T. Singh and P. Scott, "Polynomial Chaos Based Method for State and Parameter Estimation," 2012 American Control Conference, Montreal, Canada, June 27-29, 2012.

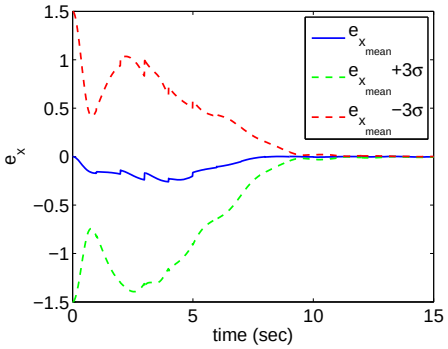

(a) Estimation Error for x ($N_m = 1$)

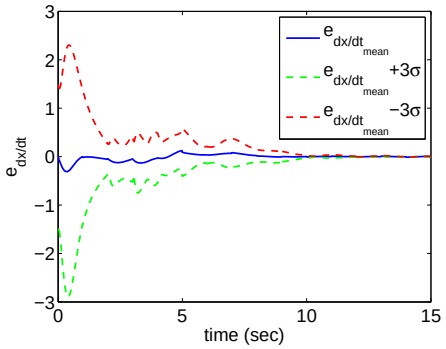

(b) Estimation Error for $\dot{x}$ ($N_m = 1$)

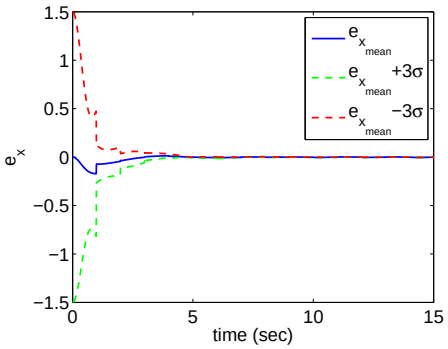

(c) Estimation Error for x ($N_m = 2$)

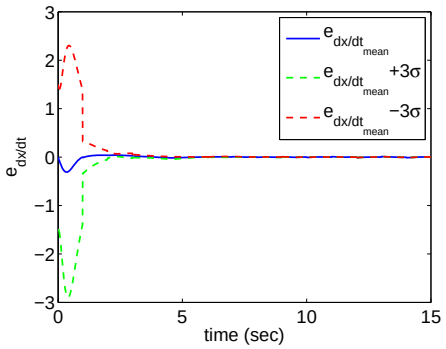

(d) Estimation Error for $\dot{x}$ ($N_m = 2$)

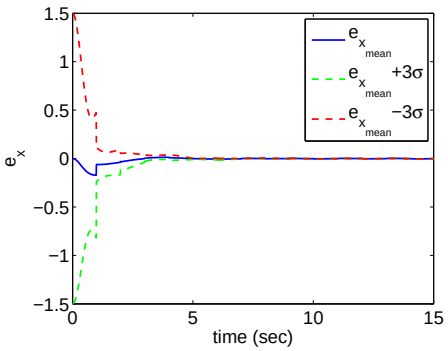

(e) Estimation Error for x ($N_m = 3$)

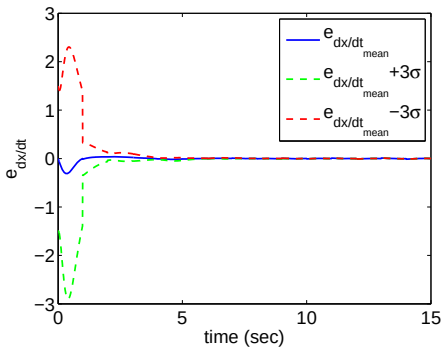

(f) Estimation Error for $\dot{x}$ ($N_m = 3$)

Figure 19: Estimation Error and 3σ Bounds for the gPC-Bayes Approximated Posterior Mean for for Duffing oscillator

7 Concluding Remarks

In summary, significant progress has been made towards characterizing non-Gaussian state density function. Two new methods adaptive Gaussian mixture model (AGMM) and conjugate unscented transformation (CUT) have been developed for this purpose. AGMM method solves the Fokker-Planck-Kolmogorov equation associated with orbital dynamics model. Furthermore, sparse approximation tools have been used to identify the Gaussian kernels which best approximate the state pdf. The CUT methodology provides efficient means to compute higher order moments of state density functions. The primary objective of CUT methodology is to find a fully symmetric sigma/cubature point set with reduced number of points that is equivalent to the set of cubature points of Gaussian quadrature product rule of same order. Equivalent to same order implies that for a polynomial of order $2m-1$ in generic N-dimensions, both the new reduced sigma point set from the proposed method known as Conjugate Unscented Transform method (CUT) and the m^N quadrature points from the Gaussian quadrature product rule result in same order of relative percentage error. In this work, a closed form expression for these new sets of point is provided to satisfy up to 8 central moments. It is shown that the proposed method provides a significant reduction in function evaluations to compute multi-dimension expectation integrals. For example, the proposed method needs only **355 and 745 function evaluations** to compute the expectation integral for a polynomial function of degree 8 in the 5- and 6-dimensional space, respectively whereas the Gaussian quadrature product rule would need **3,125 and 15,625 function evaluations** for the same 5- and 6-dimensional space respectively. Finally, optimal control problem is posed to optimize sensor locations and other modalities to better track a target object. The main highlight of this work is to compute information theoretic metrics corresponding to non-Gaussian target state pdfs to describe the current situation of the target state.

AFOSR Deliverables Submission Survey

Response ID:3735 Data

1.

1. Report Type

Final Report

Primary Contact E-mail
Contact email if there is a problem with the report.

psingla@buffalo.edu

Primary Contact Phone Number
Contact phone number if there is a problem with the report

716-645-1429

Organization / Institution name

University at Buffalo

Grant/Contract Title
The full title of the funded effort.

(YIP) Information Collection and Fusion for Space Situational Awareness

Grant/Contract Number
AFOSR assigned control number. It must begin with "FA9550" or "F49620" or "FA2386".

FA9550-11-1-0012

Principal Investigator Name
The full name of the principal investigator on the grant or contract.

Dr. Puneet Singla

Program Manager
The AFOSR Program Manager currently assigned to the award

Dr. Julie Moses

Reporting Period Start Date

04/01/2011

Reporting Period End Date

03/31/2014

Abstract

A significant progress has been made towards characterizing non-Gaussian state density function. Two new methods adaptive Gaussian mixture model (AGMM) and conjugate unscented transformation (CUT) have been developed for this purpose. AGMM method solves the Fokker-Planck-Kolmogorov equation associated with orbital dynamics model. Furthermore, sparse approximation tools have been used to identify the Gaussian kernels which best approximate the state pdf. The CUT methodology provides efficient means to compute higher order moments of state density functions. The primary objective of CUT methodology is to find a fully symmetric sigma/cubature point set with reduced number of points that is equivalent to the set of cubature points of Gaussian quadrature product rule of same order. Equivalent to same order implies that for a polynomial of order 2m-1 in generic N-dimensions, both the new reduced sigma point set from the proposed method known as Conjugate Unscented Transform method (CUT) and the m^N quadrature points from the Gaussian quadrature product rule result in same order of relative

percentage error. In this work, a closed form expression for these new sets of point is provided to satisfy up to 8 central moments. It is shown that the proposed method provides a significant reduction in function evaluations to compute multi-dimension expectation integrals. For example, the proposed method needs only 355 and 745 function evaluations to compute the expectation integral for a polynomial function of degree 8 in the 5- and 6-dimensional space, respectively whereas the Gaussian quadrature product rule would need 3,125 and 15,625 function evaluations for the same 5- and 6-dimensional space respectively. Finally, optimal control problem is posed to optimize sensor locations and other modalities to better track a target object. The main highlight of this work is to compute information theoretic metrics corresponding to non-Gaussian target state pdfs to describe the current situation of the target state.

Distribution Statement

This is block 12 on the SF298 form.

Distribution A - Approved for Public Release

Explanation for Distribution Statement

If this is not approved for public release, please provide a short explanation. E.g., contains proprietary information.

SF298 Form

Please attach your SF298 form. A blank SF298 can be found here. Please do not spend extra effort to password protect or secure the PDF, we want to read your SF298. The maximum file size for SF298's is 50MB.

AFD-070820-035.pdf

Upload the Report Document. The maximum file size for the Report Document is 50MB.

FinalReport2014.pdf

Upload a Report Document, if any. The maximum file size for the Report Document is 50MB.

Archival Publications (published) during reporting period:

K. Vishwajeet, P. Singla and M. Jah, "Nonlinear Uncertainty Propagation for Perturbed Two-Body Orbits,'' AIAA Journal of Guidance, Control and Dynamics, Accepted, January 2014,DOI: 10.2514/1.G000472.

K. Vishwajeet and P. Singla, "Adaptive Split and Merge Technique for Gaussian Mixture Models to Solve Kolmogorov Equation," 2014 American Control Conference, Portland, OR, June 4–6, 2014.

K. Vishwajeet and P. Singla, "Adaptive Split and Merge Algorithm for Gaussian Mixture Models," 2013 Astrodynamics Specialist Conference, Hilton Head, North Carolina.

K. Vishwajeet and P. Singla, "Sparse Approximation Based Gaussian Mixture Model Approach for Uncertainty Propagation for Nonlinear Systems," 2013 American Control Conference, Washington D.C.

K. Vishwajeet "Adaptive Gaussian Mixture Model for Uncertainty Propagation Through Perturbed Two-Body Model," M.S. thesis, Department of Mechanical & Aerospace Engineering, University at Buffalo, Buffalo, NY, August 2013. (Best M.S. Thesis Award from NAGS).

G. Terejanu, P. Singla, T. Singh and P. Scott, "Adaptive Gaussian Sum Filter for Nonlinear Bayesian Estimation," IEEE Transactions on Automatic Control, Vol. 56, Issue 9, pp. 2151–2156, Sep. 2011, DOI: 10.1109/TAC.2011.2141550.

N. Adurthi, and P. Singla, "A Conjugate Unscented Transformation Based Approach for Accurate Conjunction Analysis," Richard Battin Special Issue of the AIAA Journal of Guidance, Control, and Dynamics, In Preparation.

N. Adurthi and P. Singla, "Principle of Maximum Entropy for Probability Density Reconstruction: An Application to the Two Body Problem," 2013 Astrodynamics Specialist Conference, Hilton Head, SC, August 2013.

N. Adhurthi, P. Singla and T. Singh, "Conjugate Unscented Transform: a novel cubature approach for nonlinear transformation of

moments in forecasting and estimation," IEEE Transactions on Automatic Control, In Review.

N. Adurthi and P. Singla, "Principle Of Maximum Entropy For Probability Density Reconstruction: An Application To The Two Body Problem," 2013 AAS/AIAA Astrodynamics Specialist Conference.

N. Adurthi, "Conjugate Unscented Transformation Approach for Filtering and Bayesian Inference," M.S. thesis, Department of Mechanical & Aerospace Engineering, University at Buffalo, Buffalo, NY, August 2013. (Best M.S. Thesis Award from NAGS).

N. Adurthi, P. Singla and T. Singh, "Conjugate Unscented Transform Rules for Uniform Probability Density Functions," 2013 American Control Conference, Washington D.C.

N. Adurthi, P. Singla and T. Singh, "Conjugate Unscented Transform and its Application to Filter- ing and Stochastic Integral Calculation," 2012 AIAA Guidance, Navigation & Control Conference, Minneapolis, MN.

N. Adurthi, P. Singla and T. Singh, "The Conjugate Unscented Transform - An Approach to Evaluate Multi-Dimensional Expectation Integrals," 2012 American Control Conference, Montre´al, Canada, June 27-June 29, 2012.

N. Adurthi, P. Singla and T. Singh, "Conjugate Unscented Transformation "Optimal Quadrature"," 2012 SIAM Conference on Uncertainty Quantification, Raleigh, NC, April 2–April 5, 2012.

N. Adurthi, and P. Singla, "A Conjugate Unscented Transformation Based Approach for Accurate Conjunction Analysis," 2014 AIAA/AAS Astrodynamics Specialist Conference, San Diego, California, 4 - 7 August 2014.

M.Mercurio,"A Non Combinatorial Approach for Efficient Conjunction Analysis," M.S.Thesis,University at Buffalo, June 2014.

M. Mercurio and P. Singla, "A Hierarchical Tree Code Based Approach for Efficient Conjunction Analysis," 2013 Astrodynamics Specialist Conference, Hilton Head, SC, August 2013.

M. Mercurio, P. Singla and A. Patra, "A Hierarchical Tree Code Based Approach for Efficient Conjunction Analysis," 2012 AIAA/AAS Astrodynamics Specialist Conference, Minneapolis, MN, Aug. 2Aug. 5, 2012.

N. Adurthi, P. Singla and M. Majji, "Optimal Sensor Tasking for Space Situational Awareness," Richard Battin Special Issue of the AIAA Journal of Guidance, Control, and Dynamics, In Preparation.

N. Adurthi, P. Singla and M. Majji, "Information theoretic Optimal Sensor management for Efficient Space surveillance," 2014 AIAA/AAS Astrodynamics Specialist Conference, San Diego, California, 4 - 7 August 2014.

N. Adurthi and P. Singla, "Information Driven Optimal Sensor Control for Efficient Target Localization and Tracking," 2014 American Control Conference, Portland, OR, June 4–6, 2014.

N. Adurthi,P. Singla and T. Singh,"Optimal Information Collection for Nonlinear systems-An Application to Multiple Target Tracking and Localization," 2013 American Control Conference, Washington D.C.

R. Madankan, P. Singla and T. Singh, "Optimal Information Collection for Source Parameter Estimation of Atmospheric Release Phenomenon," 2014 American Control Conference, Portland, OR, June 4–6, 2014.

K. Vishwajeet, N. Adurthi and P. Singla, "Optimal Information Collection for Space Situational Awareness," 2014 SIAM Conference on Uncertainty Quantification, Savannah, GA, March 31–April 3, 2014.

N. Adurthi, R. Madankan and P. Singla, "Optimal Information Trajectory Design for Dynamic State Estimation," 2014 SIAM Conference on Uncertainty Quantification, Savannah, GA, March 31–April 3, 2014.

R. Madankan, P. Singla, T. Singh and P. Scott, "Polynomial Chaos Based Method for State and Parameter Estimation," AIAA

Journal of Guidance, Control and Dynamics, Vol. 36, No. 4 (2013), pp. 1058-1074, July 2013, DOI: 10.2514/1.58377.

R. Madankan, P. Singla, T. Singh and P. Scott, "Polynomial Chaos Based Method for State and Pa- rameter Estimation," 2012 American Control Conference, Montreal, Canada, June 27-29, 2012.

Changes in research objectives (if any):

None

Change in AFOSR Program Manager, if any:

Program manager was changed in 2012 from Dr. Kent Miller to Dr. Julie Moses

Extensions granted or milestones slipped, if any:

none

AFOSR LRIR Number

LRIR Title

Reporting Period

Laboratory Task Manager

Program Officer

Research Objectives

Technical Summary

Funding Summary by Cost Category (by FY, $K)

	Starting FY	FY+1	FY+2
Non-Military Government Personnel Costs			
In-house Contractor Costs			
Travel (Be Specific)			
Training (Be Specific)			
Supplies			
Other Expenses (Be Specific)			
Total Resource Requirements			

Report Document

Appendix Documents

2. Thank You

E-mail user

Jun 30, 2014 12:41:44 Success: Email Sent to: psingla@buffalo.edu

Response Location

Country:	United States
Region:	NY
City:	Buffalo
Postal Code:	14260
Long & Lat:	Lat: 42.768398284912, Long:-78.887100219727